



HAL
open science

Genome scans on experimentally evolved populations reveal candidate regions for adaptation to plant resistance in the potato cyst nematode *Globodera pallida*.

Delphine Eoche-Bosy, Matthieu Gautier, Magali Esquibet, Fabrice Legeai, Anthony Bretaudeau, Olivier Bouchez, Sylvain Fournet, Eric Grenier, Josselin Montarry

► To cite this version:

Delphine Eoche-Bosy, Matthieu Gautier, Magali Esquibet, Fabrice Legeai, Anthony Bretaudeau, et al.. Genome scans on experimentally evolved populations reveal candidate regions for adaptation to plant resistance in the potato cyst nematode *Globodera pallida*.. *Molecular Ecology*, 2017, 26 (18), pp.4700-4711. 10.1111/mec.14240 . hal-01605681v2

HAL Id: hal-01605681

<https://inria.hal.science/hal-01605681v2>

Submitted on 30 Aug 2017

HAL is a multi-disciplinary open access archive for the deposit and dissemination of scientific research documents, whether they are published or not. The documents may come from teaching and research institutions in France or abroad, or from public or private research centers.

L'archive ouverte pluridisciplinaire **HAL**, est destinée au dépôt et à la diffusion de documents scientifiques de niveau recherche, publiés ou non, émanant des établissements d'enseignement et de recherche français ou étrangers, des laboratoires publics ou privés.

1 **Genome scans on experimentally evolved populations reveal candidate**
2 **regions for adaptation to plant resistance in the potato cyst nematode**
3 ***Globodera pallida***

4

5 D. EOCHE-BOSY¹, M. GAUTIER^{2,3}, M. ESQUIBET¹, F. LEGEAI^{4,5}, A. BRETAUDEAU^{4,6},
6 O. BOUCHEZ^{7,8}, S. FOURNET¹, E. GRENIER¹ and J. MONTARRY¹

7

8 ¹IGEPP, INRA, Agrocampus Ouest, Université de Rennes 1, 35650, Le Rheu, France

9 ²CBGP, INRA, IRD, CIRAD, Montpellier SupAgro, 34988, Montferrier-sur-Lez, France

10 ³IBC, 34095, Montpellier, France

11 ⁴IGEPP, BIPAA, INRA, Agrocampus Ouest, Université de Rennes 1, 35042, Rennes, France

12 ⁵IRISA, GenScale, INRIA, 35042, Rennes, France

13 ⁶IRISA, GenOuest COre Facility, INRIA, 35042, Rennes, France

14 ⁷GeT-PlaGe, Genotoul, INRA, 31326, Castanet-Tolosan, France

15 ⁸GenPhySE, Université de Toulouse, INRA, INPT, ENVT, 31326, Castanet-Tolosan, France

16

17 **Keywords** evolve and resequence; experimental evolution; Pool-Seq; population
18 genomics; selection; virulence

19

20 Correspondence: Josselin Montarry, IGEPP, INRA, Agrocampus Ouest, Université de Rennes
21 1, 35650, Le Rheu, France; Fax: +33 2 23 48 51 50; E-mail: josselin.montarry@inra.fr

22

23 Running title: Molecular signatures of adaptation to resistance

24 **Abstract**

25 Improving resistance durability involves to be able to predict the adaptation speed of
26 pathogen populations. Identifying the genetic bases of pathogen adaptation to plant
27 resistances is a useful step to better understand and anticipate this phenomenon. *Globodera*
28 *pallida* is a major pest of potato crop for which a resistance QTL, *GpaV_{vm}*, has been identified
29 in *Solanum vernei*. However, its durability is threatened as *G. pallida* populations are able to
30 adapt to the resistance in few generations. The aim of the present study was to investigate the
31 genomic regions involved in the resistance breakdown by coupling experimental evolution
32 and high density genome scan. We performed a whole genome resequencing of pools of
33 individuals (Pool-Seq) belonging to *G. pallida* lineages derived from two independent
34 populations having experimentally evolved on susceptible and resistant potato cultivars.
35 About 1.6 million SNPs were used to perform the genome scan using a recent model testing
36 for adaptive differentiation and association to population-specific covariables. We identified
37 275 outliers and 31 of them, which also showed a significant reduction of diversity in adapted
38 lineages, were investigated for their genic environment. Some candidate genomic regions
39 contained genes putatively encoding effectors and were enriched in SPRYSECs, known in
40 cyst nematodes to be involved in pathogenicity and in (a)virulence. Validated candidate SNPs
41 will provide a useful molecular tool to follow frequencies of virulence alleles in natural *G.*
42 *pallida* populations and define efficient strategies of use of potato resistances maximizing
43 their durability.

44

45 **Introduction**

46 Because of the threat caused by crop pathogens to global food security, control methods to
47 limit yield losses and maintain sustainable productions are needed. If pesticides have been
48 successfully employed for years, the current societal and political demand for a reduction of
49 their use is strong. In most cases, resistant cultivars are now the chosen alternative, as they
50 can be highly effective, organism-specific, economically and environmentally sustainable.
51 However, this control method can be limited by evolutionary capacities of targeted pathogens,
52 which can adapt to plant resistances (McDonald & Linde 2002). Resistance breakdowns have
53 been documented in a wide range of crop pathogens, such as virus, bacteria, nematodes, fungi
54 or oomycetes (e.g., Castagnone-Sereno 2002; McDonald & Linde 2002; Janzac *et al.* 2009),
55 whereas the development of resistant cultivars is a long process, in the order of decades, *i.e.*
56 usually longer than the time needed for pathogen populations to overcome resistances.
57 Consequently, the design of strategies allowing an increase in resistance durability has been a
58 major goal in plant pathology research over the last 50 years, especially as resistance genes or
59 QTLs remain a scarce resource. To be efficient, such strategies have to integrate knowledge
60 on the adaptation of pathogen populations to the selective pressure imposed by the resistant
61 plant. Consequently, a significant step towards a better management of resistance durability
62 could be taken by identifying the genetic determinants of adaptation to plant resistances,
63 which would represent direct predictors allowing to link dynamics and genetics of resistance
64 breakdown.

65 Plant-parasitic nematodes are major agricultural pathogens causing severe damages in
66 crops worldwide (Nicol *et al.* 2011), but sources of resistance against them remain scarce.
67 Several studies have been conducted to optimize the management of these resistances (Djian-
68 Caporalino *et al.* 2014; Barbary *et al.* 2015). Cyst nematodes are among the most

69 economically damaging plant-parasitic nematodes. Over the last few years, increased
70 knowledge about characteristics of cyst nematode populations allowed to better predict the
71 global evolutionary potential of these populations. In particular it was showed that cyst
72 nematode populations represent a real threat to the durability of plant resistances due to an
73 important passive dispersion (Picard *et al.* 2004; Plantard & Porte 2004; Alenda *et al.* 2014)
74 and favored expression of recessives virulence genes due to inbreeding (Montarry *et al.*
75 2015). The adaptation speed of nematode populations would also be modulated by the number
76 and the nature of genetic mutations required to overcome the plant resistance, and by the
77 presence and, if any, the frequency, of virulent individuals in fields.

78 The cyst nematode *Globodera pallida* (Stone) is a major pest of potato crop (Oerke *et*
79 *al.* 1994; van Riel & Mulder 1998) and *Solanum vernei*, a wild potato species, is an
80 interesting source of resistance against *G. pallida* as it is highly effective. The resistance,
81 which leads to the development of most nematodes into adult males, is explained at 61% by
82 the major QTL *GpaV_{vrn}* mapped on the potato chromosome V (Roupe van der Voort *et al.*
83 2000). This source of resistance is to date the only one exploited in commercial potato
84 cultivars at the European level. The resistant cultivar Iledher, carrying *GpaV_{vrn}*, has been
85 registered in 2009 in the French catalogue as the first cultivar showing a high level of
86 resistance to *G. pallida*. However, Fournet *et al.* (2013) highlighted that *G. pallida*
87 populations were able to completely overcome the resistance of Iledher in only few
88 generations in experimental evolution. Identifying the determinants of virulence thus appears
89 to be crucial to better anticipate the speed of adaptation of *G. pallida* populations.

90 In organisms with relatively small genomes, such as RNA viruses with 10-15 kb
91 genomes, it is possible since several years to sequence the entire genome and to directly
92 compare sequences of virulent and avirulent strains in order to find the mutation responsible

93 for resistance adaptation (Meshi *et al.* 1988; Díaz *et al.* 2004; Ayme *et al.* 2006; Mardis 2008;
94 Janzac *et al.* 2010). However, this approach cannot be considered in eukaryotic organisms
95 whose genomes range from one to hundreds of thousands megabases. Genome scans
96 represent an efficient alternative to target genomic regions involved in adaptation in such
97 organisms, as they analyze genome-wide variations at the light of theoretical predictions
98 about the effects of selection, in order to detect locus specific signatures of positive
99 directional selection (Luikart *et al.* 2003; Storz 2005). Despite their strong potential to
100 elucidate the genetic bases of adaptation, genome scans have never been used to identify the
101 determinants of virulence in nematodes. However, Bekal *et al.* (2015) recently opened the
102 way for population genomic approach in cyst nematodes. They performed a whole genome
103 allelic imbalance analysis of SNP in *Heterodera glycines* inbred lines grown in the laboratory
104 for over 30 generations on resistant and susceptible soybean plants. This study revealed two
105 new candidate virulence genes: *HgBioB*, a gene encoded biotin synthase and *HgSLP-1*, a gene
106 that appears to have entered *H. glycines* genome via horizontal gene transfer and which
107 encode a protein containing a putative SNARE domain. Virulence is based on sequence
108 polymorphisms for the first gene and on a reduced copy number for the second gene. In
109 potato cyst nematodes, (a)virulence genes known to date were identified only through
110 candidate gene approaches. In *Globodera rostochiensis*, the venom allergen Gr-VAP1 was
111 identified as an avirulence gene product triggering a cell death response in tomato
112 (*Lycopersicon esculentum*) plants containing the *Cf-2* and *Rcr3pim* resistant genes (Lozano-
113 Torres *et al.* 2012, 2014). In *G. pallida*, only one avirulence gene, *Gp-RBP-1*, coding for a
114 SPRYSEC which interacts with the GPA2 resistant protein in potato, has been described
115 (Sacco *et al.* 2009). Virulence is due to a single amino-acid polymorphism, however this
116 mutation is widely distributed in European populations (Carpentier *et al.* 2012) and therefore

117 potato carrying *Gpa2* resistance gene is of very limited interest for control of *G. pallida*. On
118 the contrary, the resistant cultivar Iledher shows a high level of resistance to a wide range of
119 European *G. pallida* populations.

120 The aim of the present study was to investigate the *G. pallida* genomic regions
121 involved in the breakdown of the resistance of potato cultivar Iledher. By analyzing
122 microsatellite data, Eoche-Bosy *et al.* (2016) already showed that a genome scan on the *G.*
123 *pallida* lineages coming from the experimental evolution performed by Fournet *et al.* (2013)
124 was feasible. Here, we took advantage of the same biological material to perform a high
125 density genome scan using data from a whole genome resequencing of pools of individuals
126 (Pool-Seq, Futschik & Schlötterer 2010; Zhu *et al.* 2012; Ferretti *et al.* 2013; Gautier *et al.*
127 2013; Schlötterer *et al.* 2014) and a recent model testing for adaptive differentiation and
128 association to population-specific covariables (BayPass, Gautier 2015).

129

130 **Materials and methods**

131 *Study system: Globodera pallida*

132 *Globodera pallida* is a gonochoristic diploid organism with obligate sexual reproduction,
133 which achieves one generation per year in European climatic conditions (Jones 1950). This
134 obligate parasite enters the plant roots as second-stage juveniles (J2) and establishes a
135 specialized feeding structure, the syncytium (Jones & Northcote 1972), which is a severe
136 nutrient sink for the plant. In this species, sex is environmentally determined and depends on
137 the size and efficiency of the syncytium (Sobczak & Golinowski 2011). Adult males leave the
138 root to mate females, which can be fertilized by several males (Green *et al.* 1970;
139 Triantaphyllou & Esbenshade 1990). After mating, the females continue to feed from the

140 syncytium and when eggs development is completed, they die and form a cyst, enclosing
141 hundreds of eggs, which can stay viable for several years in soils.

142 The genome of *G. pallida* has been recently sequenced (Gpal.v1.0, Cotton *et al.* 2014).
143 It is available as an assembly of 124.7 Mb in 6,873 scaffolds, with a N50 of 122 kb and a GC
144 content of 36.7% (Cotton *et al.* 2014). Combining transcriptomic data with manual curation, a
145 total of 16,419 genes were predicted. The genome of *G. rostochiensis* has also been recently
146 sequenced (nGr.v1.0, Eves-van den Akker *et al.* 2016) and could be a more accurate
147 representation of a *Globodera* genome, as suggested by its higher completeness and low level
148 of gene duplication. This genome is available as an assembly of 95.9 Mb in 4,377 scaffolds,
149 with a N50 of 88 kb and a GC content of 38.1%. Annotation of *G. rostochiensis* genome
150 could also be of better quality as a manual annotation phase followed the initial phase of
151 automated annotation, resulting in the prediction of 14,378 genes.

152

153 *Selection of virulent and avirulent G. pallida lineages*

154 This study relies on the biological material coming from the experimental evolution
155 performed by Fournet *et al.* (2013). Briefly, nematode lineages were established from cysts of
156 two French natural *G. pallida* populations, SM (near Saint-Malo, Brittany, north-western
157 France) and N (from the island of Noirmoutier, western France) coming from infested fields
158 (Fig. 1). The lineages used here were obtained by rearing both populations during eight
159 successive cycles (*i.e.* eight generations) on the susceptible potato cultivar Désirée (D) and on
160 the resistant cultivar Iledher (I). The present study was conducted with the eighth generation
161 of the four lineages: two lineages adapted to the resistance of Iledher (named hereafter SMI
162 and NI), and two lineages which remained unadapted (named hereafter SMD and ND).

163

164 *Pool sequencing*

165 As the amount of DNA in a single *G. pallida* individual is very low, pooling individuals from
166 a same lineage was an efficient way to increase the amount of DNA while allowing the
167 accurate estimation of population allele frequencies (e.g., Gautier *et al.* 2013). To accurately
168 represent the genetic variability of each lineage, we chose to sample individuals from
169 different cysts, rather than different individuals from a same cyst, to constitute the pools. We
170 therefore sampled 300 cysts in each lineage, which was the maximum available, and crushed
171 them individually in sterile water. Two J2 (siblings) were sampled from each cyst and
172 attributed to two different pools, resulting in two pools of 300 individuals for each lineage,
173 *i.e.* two biological replicates. Water in samples was then vacuum-evaporated in a heated
174 Speed Vac Concentrator (MiVac, Genevac Ltd., Ipswich, UK). As the cuticle of the nematode
175 could prevent the lysis of tissues by the proteinase K, samples were stored at -80°C during
176 two hours and then rapidly heated at ambient temperature, just before DNA extraction. DNA
177 was extracted directly from each pool using Qiagen DNeasy Blood and Tissue Kit (Qiagen,
178 Hilden, Germany) following the manufacturer's instructions. A pooled DNA extraction has
179 been favored over an individual DNA extraction following by a pooling of the DNA in
180 equimolar proportions because this last strategy can lead to heterogeneity in the amount of
181 each individual DNA due to measurement (poor estimations of individuals DNA
182 concentration) or pipetting errors (Gautier *et al.* 2013). Extracted genomic DNA was
183 quantified using a Qubit® 2.0 Fluorometer (Invitrogen, Carlsbad, CA, USA) and quality was
184 estimated using a Nanodrop® ND-2000 Spectrophotometer (Thermo Fisher Scientific,
185 Wilmington, DE, USA). The DNA samples conformed to the required purity criteria
186 (A_{260}/A_{230} and $A_{260}/A_{280} > 1.8$) for gDNA library preparation for sequencing, but not to
187 the required concentration criterion, as the amount of DNA obtained from a 300 individuals

188 pool was still very low (*i.e.* 17 ng of DNA per pool on average). Paired-end libraries were
189 therefore constructed from the totality of DNA available in each pool (*i.e.* each biological
190 replicate in each lineage) contained in 100 μ L AE buffer (Qiagen), using the TruSeq Nano
191 DNA Sample Preparation Kits (Illumina, San Diego, CA, USA), according to the
192 manufacturer's instructions. Briefly, DNA was fragmented using a Covaris M220
193 ultrasonicator (Covaris, Woburn, MA, USA) and, after a purification step, end repaired. A
194 bead-based size selection was performed, then DNA was A-tailed and ligated to indexed
195 sequencing adapters (60 bp on each side), each biological replicate being identified by a
196 different index. After a double-purification, libraries were enriched by eight PCR cycles,
197 followed by a final purification. Library profiles were controlled using a DNA High
198 Sensitivity chip on a BioAnalyzer 2100 (Agilent Technologies, Santa Clara, CA, USA),
199 showing that the average size of the eight libraries was 513 bp (*i.e.* average insert size of 493
200 bp). Libraries were then quantified by qPCR on ABI7900HT (Applied Biosystems) in order to
201 pool them in equimolar proportions. The final pool was again quantified by qPCR on
202 ABI7900HT in order to load on each lane a volume corresponding to a DNA concentration of
203 8 pM. In order to sequence the eight libraries at an expected 150X coverage depth, four lanes
204 were necessary. Sequencing was performed on an Illumina HiSeq™ 2500 platform (Illumina).
205 Three lanes were sequenced with HiSeq v4 reagent kits (HiSeq PE Cluster Kit v4 and HiSeq
206 SBS Kit v4, Illumina) providing 2x125 bp paired-end reads and the fourth lane was
207 sequenced with TruSeq v3 reagents kit (TruSeq PE Cluster Kit v3 and TruSeq SBS Kit v3,
208 Illumina) providing 2x100 bp paired-end reads. Libraries preparation and sequencing were
209 performed at the GeT-PlaGe France Genomics sequencing platform (Toulouse, France). All
210 the obtained data were submitted to the BBRIC Archive network ([https://bbri-
archive.toulouse.inra.fr/web/index.html](https://bbri-
211 archive.toulouse.inra.fr/web/index.html)) in Project Gpool.

212

213 *Mapping and SNP calling*

214 Reads from the 64 fastq files (4 lineages x 2 biological replicates x 4 lanes x 2 (paired-end))
215 were aligned to the *G. pallida* reference genome using Bowtie2 version 2.1.0 (Langmead *et*
216 *al.* 2009; Langmead & Salzberg 2012) with default parameters. Duplicate reads were removed
217 using Picard version 1.122.0 (<http://broadinstitute.github.io/picard/>) and remaining reads were
218 realigned around indels using Realigner Target Creator and Indel Realigner from the Genome
219 Analysis Toolkit, GATK version 2.8.0 (McKenna *et al.* 2010; DePristo *et al.* 2011; Van der
220 Auwera *et al.* 2013). The 32 BAM files obtained were merged in a single mpileup file using
221 SAMtools MPileup version 0.1.19 (Li *et al.* 2009) with minimum mapping quality and
222 minimum base quality set to 20. The whole previous workflow was performed on the Galaxy
223 platform (<https://galaxyproject.org/>, Blankenberg *et al.* 2010). The mpileup file was further
224 processed to perform SNP calling and derive read counts for each alternative base, after
225 discarding bases with a Base Alignment Quality score below 25. Genomic positions kept in
226 the dataset had to show only two different bases across all the samples, however, the tri-
227 allelic positions for which the third allele was represented by only one read were included in
228 the analysis as bi-allelic SNPs (after filtering the third allele as a sequencing error). To
229 evaluate the reproducibility of the sequencing results across the technical replicates
230 (sequencing lanes), we carried out a Principal Component Analysis (PCA) based on the allele
231 frequency counts (Fig. S1, Supporting information). A last filtering step based on the
232 coverage and the minimum allele count (MAC) was performed: a SNP was kept in the dataset
233 if i) it had a coverage of more than 30 reads and less than 300 reads (corresponding
234 approximately to the 95% percentile of the empirical coverage distribution) in each sample
235 and ii) the minor allele was represented by at least two reads in two different pool samples.

236

237 *Genome scan for adaptive divergence and association with the virulent/avirulent status*

238 To detect genomic signatures of selection, we used the package BayPass version 2.1 (Gautier
239 2015) that provides a reimplementation of the Bayesian hierarchical model initially proposed
240 by Coop *et al.* (2010) and includes several extensions that improve accuracy and decision
241 criteria. The underlying BayPass framework allows both to identify overly differentiated
242 SNPs (candidate for adaptive selection) in a robust fashion, through the computation of the
243 XtX genetic differentiation statistics (Günther & Coop 2013), and to perform genome-wide
244 association with population-specific covariables. The underlying models explicitly account
245 for the covariance structure among the population allele frequencies that originates from the
246 shared history of the populations under study, through the estimation of the population
247 covariance matrix Ω , which renders the identification of SNPs subjected to selection less
248 sensitive to the confounding effect of demography (Bonhomme *et al.* 2010; Günther & Coop
249 2013). BayPass is generic enough to be suited for the analyses of data from experimental
250 evolution in which the allele frequency covariance structure is simpler, and can handle data
251 derived from Pool-Seq experiments (Gautier 2015).

252 The allele count dataset was analyzed under all the models implemented in BayPass
253 with all the parameter set to default, considering the virulence/avirulence status (coded as a
254 binary variable with value -1 and 1 respectively) of each sample for the association analysis.
255 First, analysis under the core model allowed to estimate the XtX for each SNP that were
256 calibrated after analyzing a pseudo-observed dataset (POD) simulated under the inference
257 model with parameters set equal to those estimated in the real data. Second, we relied on the
258 Bayes Factor (BF) calculated under the auxiliary covariate model to evaluate association of
259 SNPs to the virulent/avirulent status of the lineages. The auxiliary covariate model involves

260 the introduction of a binary auxiliary variable to classify each locus as associated or not. This
261 allows to easily compute Posterior Inclusion Probability (and BF) for each locus while
262 explicitly accounting for multiple testing issues. For each SNP, the Bayes Factor (denoted
263 BF_{mc} as in Gautier 2015) was expressed in deciban units (dB) via the transformation $10 \log_{10}$
264 (BF). As a decision rule, we then followed the popular Jeffreys' rule (Jeffreys 1961) that
265 quantifies the strength of evidence (here in favor of association of the SNP with the
266 covariable) as 'strong' when $10 \text{ dB} < BF < 15 \text{ dB}$, 'very strong' when $15 \text{ dB} < BF < 20 \text{ dB}$
267 and 'decisive' when $BF > 20 \text{ dB}$.

268 Three independent BayPass analyses were carried out for each model, giving different
269 values to initial seed of the (pseudo-) Random Number Generator. Under the core model in
270 particular, the posterior estimates of Ω were found almost identical with a FMD distance
271 (Förstner & Moonen 2003) between each pair of matrices always lower than 0.01. For
272 prioritization purposes, only SNPs that were overly differentiated if $XtX > 1\%$ POD
273 significance threshold and if $BF_{mc} > 20$ in the three independent analyses were further
274 considered as candidate.

275 As we were interested in identifying genomic regions involved in the adaptation to
276 Iledher, we precisely had to consider only SNPs showing footprints of selection in the Iledher
277 lineages (SMI and NI) and not in the Désirée lineages. It is in fact possible to pinpoint
278 genomic regions involved in host adaptation (rather than resistance adaptation), which can
279 occur both in nematode lineages having evolved on Iledher and in the ones having evolved on
280 Désirée, as highlighted in Eoche-Bosy *et al.* (2016). For this purpose, we used the lnRH test
281 (Kauer *et al.* 2003; Schlötterer & Dieringer 2005). LnRH is traditionally used for
282 microsatellite datasets, but as it is not based on a particular mutation model (Kauer *et al.*
283 2003), it can also be applied to SNP datasets (Mc Evoy *et al.* 2006; Vasemägi *et al.* 2012).

284 This test, based on the assumption that markers linked to loci under selection will show
285 reduced levels of diversity within populations (Schlötterer & Dieringer 2005), uses the
286 expected heterozygosity H to compute the $\ln RH$ statistics. We merged allelic counts of
287 biological replicates and derived from it allelic frequencies at each SNP in SMI, SMD, NI and
288 ND. We computed the $\ln RH$ statistic for each locus in lineage pairs SMI/SMD and NI/ND by
289 calculating the natural logarithm (\ln) of the gene diversity ratio $[(1/(1-H_{\text{lineage1}}))^2-1] / [(1/(1-$
290 $H_{\text{lineage2}}))^2-1]$. For lineages with monomorphic loci, one different allele was added to one
291 individual, as null values of heterozygosity prevent the estimation of $\ln RH$ due to division by
292 zero (Kauer *et al.* 2003). $\ln RH$ estimates were standardized to obtain a mean of 0 and a
293 standard deviation of 1. As the $\ln RH$ is approximately normally distributed under the null
294 hypothesis of neutrality (Schlötterer & Dieringer 2005), loci with $\ln RH$ values lower than -
295 1.96 were considered outliers at the 0.05 threshold, indicating reduced variability in SMI and
296 NI lineages as compared to SMD and ND, respectively. Only outliers in both $\ln RH$ pairwise
297 comparisons were considered, and common outliers to BayPass and $\ln RH$ were retained to
298 further investigation of their genic environment.

299

300 *Genic environment of outlier loci*

301 We searched for predicted genes located in a window of 120-kb around outlier loci (60-kb
302 either side) in the annotated *G. pallida* genome. The choice of this value was based on the
303 AFLP-based genetic linkage map of *G. rostochiensis* giving a physical:genetic distance ratio
304 of 120 kb.cM⁻¹ (Roupe van der Voort *et al.* 1999), as no data on the extent of recombination
305 and linkage disequilibrium was available in *G. pallida*. As the majority of virulence factors
306 identified in plant parasitic nematodes are effectors (Haegeman *et al.* 2012; Mitchum *et al.*
307 2013), we searched as a priority for genes coding for secreted proteins, *i.e.* harboring N-

308 terminal signal peptides in the predicted proteins, using SIGNALP v4.1 (Petersen *et al.* 2011).
309 We also performed a BLAST search of the predicted genes against the annotated *G.*
310 *rostochiensis* genome in order to potentially obtain more precise information on their
311 functional annotation. Eves-van den Akker *et al.* (2016) identified in *G. rostochiensis* and
312 subsequently in *G. pallida* genomes a dorsal gland promoter element motif, termed DOG
313 Box, which may be a strong predictor of secretion, and thus likely effector function. We thus
314 searched for the presence of the predicted genes identified around outlier loci in the *G. pallida*
315 putative DOG effectors list established by Eves-van den Akker *et al.* (2016).

316

317 **Results**

318 *Sequencing, mapping and SNP calling*

319 Sequencing was carried out on duplicates of the lineages SMI, SMD, NI and ND. Despite the
320 low amount of DNA used for each lineage, the generated sequencing data corresponded to the
321 expectations from a quantitative and qualitative point of view. Sequencing produced two
322 billion reads, *i.e.* 62.5 million reads/sample (biological replicate)/lane, and 76% mapped on
323 the *G. pallida* reference genome, but 24% of these mapping reads mapped more than once on
324 the genome. Duplicate filtering resulted in removing 13.5% of mapped reads. Remaining
325 reads covered 95% of the ungapped assembly at an average depth of 34X/sample/lane.
326 Processed mpileup contained 2,383,040 SNPs. PCA based on the allele frequency counts
327 showed that the main axes of variation of genetic variability across the different samples were
328 clearly associated with (i) the population origin and (ii) the virulence status. A very low
329 variation was observed among the sequencing replicates in each pool sample. This prompted
330 us to merge allele count data from the four sequencing replicates (lanes) for each of the eight
331 pool samples (Fig. S1, Supporting information). The final dataset filtered on coverage and

332 MAC consisted of read count data for 1,631,158 SNPs in the eight different selected lineages,
333 corresponding to a density of polymorphic sites of 16/kb on average.

334

335 *Genome scan for adaptive divergence and association with the virulent/avirulent status*

336 Analysis of the dataset under the BayPass core model allowed us to estimate the scaled
337 covariance matrix of population allele frequencies Ω that quantifies the genetic relationship
338 among each pairs of populations. The resulting estimates of Ω accurately reflected the known
339 structure between samples, *i.e.* a clustering at the higher level by population geographical
340 origin, then by the virulence status and finally by biological replicate within each lineage (Fig.
341 2). XtX for each SNP were also estimated and calibrated by analyses of a POD containing
342 1,600,000 SNPs. At the 1% POD significance threshold, about 33,000 SNPs were identified
343 as overly differentiated (Fig. 3). However, analysis under the auxiliary covariate model
344 drastically reduced this outlier list, as less than 400 had also a $BF_{mc} < 20$ (355, 361 and 357
345 SNPs in each analysis, respectively) (Fig. 3). Overall, 275 outliers were shared by the three
346 analyses (outlier loci found in only one or two analyses actually exhibited XtX and/or BF_{mc}
347 values close to the thresholds, which explains that they were not found in all analyses).
348 Among these 275 SNPs showing an increase of genetic differentiation between Iledher and
349 Désirée lineages, 31 of them also showed a decrease of genetic diversity in both SMI and NI
350 lineages (Fig. 4) as identified by lnRH.

351

352 *Genic environment of outlier loci*

353 The 31 selected outlier loci were distributed on 23 different scaffolds. Among these outlier
354 loci for which the genic environment has been investigated, three outliers were located on
355 scaffolds which do not harbor any predicted gene, 16 were located in intergenic area and 12

356 were directly located into genes (Table S2, Supporting information). Among the latter, five
357 were located in exons, and four of them corresponded to synonymous mutations. The outlier
358 SNP located on the scaffold 1777 corresponded to a non-synonymous mutation that changes
359 an arginine into a histidine in GPLIN_001438500, which is annotated as a transcribed
360 hypothetical protein. Despite the fragmentation of the *G. pallida* genome in numerous
361 scaffolds that precluded a clear analysis of the physical distances among most of the identified
362 outliers, it appeared that several outlier loci were sometimes found in the same scaffold. The
363 most significant was the scaffold 988 which contains four outlier SNPs close to each other (<
364 200 bp). Four other scaffolds (44, 85, 182 and 283) harbored outlier SNPs close to each other
365 (< 200 bp) and a fifth scaffold (66) harbored also two outlier SNPs but that are 75 kb apart.
366 The number of outlier SNPs found in a scaffold was not dependent on the size of this
367 scaffold: for instance, scaffold 988, which is one of the smallest scaffold of interest identified,
368 contains four outlier loci. Overall, 258 predicted genes were identified in a 120-kb window
369 around the 31 outlier loci (Table S2, Supporting information). About 47% (121) of them have
370 unknown function in *G. pallida*, but 15 harbored a signal peptide, indicating that they
371 potentially encode for secreted proteins, and one, GPLIN_000314000, is similar to an effector
372 in *G. rostochiensis* (Cotton *et al.* 2014). Fourteen predicted genes with known functions also
373 harbored a peptide signal. Fifteen genes coding for proteins harboring a SPRY domain were
374 found at the proximity of eight outlier loci, and three of them were paralog of SPRYSECs
375 (Secreted protein with a SPRY domain), which are known in nematodes of the genus
376 *Globodera* to be involved in pathogenicity but also in (a)virulence (Rehman *et al.* 2009;
377 Sacco *et al.* 2009). Two of them, located on scaffolds 182 and 782, were paralog of RBP-1,
378 the only virulence gene identified in *G. pallida* (Sacco *et al.* 2009; Carpentier *et al.* 2012). It
379 is likely that some of the other genes coding for proteins harboring a SPRY domain could

380 actually be SPRYSECs, the absence of signal peptide being not ascertained as they are 5'
381 truncated (N's region) in the reference genome. Other genes were also interesting as they
382 encode proteins which have functions linked to *G. pallida* pathogenicity, e.g., cell wall
383 modifying proteins, or they encode proteins which are known to be secreted by the dorsal
384 pharyngeal gland of *G. pallida*. The pharyngeal glands are cells in which effectors are
385 produced, and thus can be regarded as a toolbox for infection (Eves-van den Akker & Birch
386 2016). Cyst nematodes have two sets, subventral and dorsal: the former are primarily active
387 while the nematode migrates through host tissue, while the latter are primarily active during
388 the sedentary parasitic stages (Endo 1987; von Mende 1997; Davis *et al.* 2000). Some genes
389 with unknown function in *G. pallida* had homologues with predicted function in *G.*
390 *rostochiensis* genome, part of them being putatively paralog of SPRYSECs or involved in
391 pathogenicity. Three predicted genes (GPLIN_000832500, GPLIN_001056700 and
392 GPLIN_001258100) harbored DOG Boxes in their promoter region, two of them having
393 unknown function and the third coding for a SPRYSEC protein.

394

395 **Discussion**

396 In this study, we investigated *Globodera pallida* genomic regions involved in the adaptation
397 to the QTL *GpaV_{vm}*, a resistance factor against this potato parasite, by performing a genome
398 scan on Pool-Seq data derived from experimentally evolved lineages, adapted or not to the
399 resistant potato cultivar Iledher.

400 Elucidating the molecular bases of virulence is a central challenge in nematology. So
401 far, a few plant-nematode interactions have been studied to characterize the molecular
402 determinants of (a)virulence. In *G. pallida*, only one virulence gene has been described
403 (Sacco *et al.* 2009; Carpentier *et al.* 2012). *A priori* methods based on candidate genes to

404 identify new or unknown virulence genes are therefore not the most adapted ones at the
405 moment. Our study is the first to exploit genome scan to target genetic bases of adaptation to
406 plant resistance in nematode populations. We demonstrated in a previous study the feasibility
407 of a genome scan approach on our specific biological material coming from short
408 experimental evolution (Eoche-Bosy *et al.* 2016), which was achieved here by the
409 identification of 275 outlier loci and 31 candidates of a strong interest among them,
410 distributed on 23 scaffolds. Several genomic regions are therefore putatively linked to
411 adaptation to the resistance of Iledher, however this number should be put in perspective with
412 respects to the moderate quality of the *G. pallida* reference genome. In fact, the genome
413 assembly is still relatively fragmented (6,873 scaffolds), which could suggest that different
414 genomic regions identified as outliers in our study could in fact form only one or a few. Eves-
415 van den Akker *et al.* (2016) highlighted that some effector islands identified in *G.*
416 *rostochiensis* genome were split across different scaffolds in *G. pallida* genome. This
417 prevents to make realistic assumptions on the number of genes that could be involved in the
418 overcoming of Iledher resistance. However, we assume that only a few virulence genes
419 should be involved as few resistance genetic factors are expected in Iledher because of the
420 major effect of the QTL *GpaV_{vm}* which is present in the potato cultivar Iledher and the fast
421 overcoming of this resistance observed in experimental evolution that support rather the view
422 of a mono- or oligogenic resistance.

423 The moderate quality of the genome involved other limitations in mapping of
424 sequencing reads, leading to the loss of a substantial part of the data. First, 24% of the
425 sequencing reads did not map on the reference genome, while in the same time, the assembly
426 contains 17% of N's and has a CEGMA completeness score of 74% for complete genes and
427 81% for partial genes (Parra *et al.* 2007; Eves-van den Akker *et al.* 2016). This suggests that a

428 large part of unmapped reads could actually belongs to the *G. pallida* genome, but
429 corresponding sequences would be absent from the assemblage. These missing sequences
430 could putatively comprise candidate genomic regions to adaptation. Second, heterozygosity of
431 the reference genome is suspected, as about 24% of the sequencing reads mapped more than
432 once on the genome, this hypothesis being supported by the difference between the length of
433 the assembly (124.7 Mb) and the estimated genome size (100 Mb). Sequencing data mapping
434 on these genomic regions were further discarded because of poor mapping score due to the
435 multiple positions mapping, and once again, genomic information about these regions and
436 their possible link to resistance adaptation were lost.

437 Pool-Seq is now commonly adopted in many studies, included population genomics
438 studies (Rubin *et al.* 2010, 2012; Clément *et al.* 2013; Ferretti *et al.* 2013; Fisher *et al.* 2013),
439 because it provides more accurate estimation of allele frequencies, at reduced sequencing and
440 library preparation costs (Futschik & Schlötterer 2010; Zhu *et al.* 2012; Gautier *et al.* 2013;
441 Rellstab *et al.* 2013; Schlötterer *et al.* 2014). Here, we emphasize the interest of using such an
442 approach for population genomic studies of non-clonal microorganisms, as it allowed to
443 increase the amount of DNA while keeping information about allele frequencies. The good
444 quality of our results also relies on library preparation protocol, which fit the
445 recommendations (Rhodes *et al.* 2014; Kofler *et al.* 2016). The TruSeq Nano DNA kit has
446 been shown to be highly accurate and even some duplicates were obtained due to the PCR
447 cycles, Kofler *et al.* (2016) showed that duplicates were also obtained with free-PCR library
448 preparation kits. Nevertheless, Kofler *et al.* (2016) highlighted the superior impact of the
449 genome quality over the library preparation protocol on the mapping quality. Numbers of
450 individuals in pools and depth of coverage used have also been determined to improve
451 sequencing results and allelic frequency estimations (Gautier *et al.* 2013; Kofler *et al.* 2016).

452 Consideration of a categorical population specific covariable in the genome scan
453 allowed us to refine the list of outlier loci. Analysis of association further conducted by
454 running the auxiliary covariate model allowed to retain only SNPs associated with the
455 virulence status of the lineages, and not those corresponding to other selective pressures (e.g.,
456 local adaptation), which helped to reduce the risk of a misleading biological interpretation, a
457 main limitation of genome scans (Pavlidis *et al.* 2012). Moreover, evaluating the reduction of
458 diversity allowed us to refine the outlier loci list to those linked only to the adaptation to the
459 resistant cultivar Iledher. A direct link between those candidate loci and the adaptation to the
460 resistance cannot yet be done at this stage. Indeed, footprints of selection detected in lineages
461 having evolved on Iledher might well be linked to adaptation to the plant resistance or to the
462 plant itself (including all its genetic background). Also, at this stage, we are unable to
463 definitively link the identified SNPs to the resistance factor $GpaV_{vm}$ or to another resistance
464 factor present in the genetic background of the cultivar Iledher. Although these different
465 situations will only be deciphering by functional validation, there is a strong possibility that at
466 least some of the candidate genomic regions identified in this study are involved in adaptation
467 to Iledher resistance and in particular to its major resistance QTL $GpaV_{vm}$.

468 Sixteen over the 31 outlier loci investigated for their genic environment have at least
469 one gene coding for a secreted protein in their neighboring region (even if all secreted
470 proteins are not effectors, all effectors are secreted protein) and several outliers are at the
471 vicinity of genes coding for proteins specifically secreted in the nematode dorsal gland.
472 Particularly, some of these secreted proteins are SPRYSECs effectors which act as a versatile
473 protein-binding platform for the nematodes to target a wide range of host proteins during
474 parasitism including plant resistance proteins (Rehman *et al.* 2009; Sacco *et al.* 2009; Diaz-
475 Granados *et al.* 2016). The fact that a considerable part of the outlier loci are found near genes

476 coding for a SPRY domain containing protein or even in or at the vicinity of SPRYSECs
477 cannot be only explained by the huge size of this family gene or the prevalence of the SPRY
478 domain in the *G. pallida* genome. In fact, 299 SPRY domain containing proteins are present
479 in the *G. pallida* genome (which can be moreover cluster into islands), *i.e.* 1 for 334 kb, and
480 30 of them are SPRYSECs, *i.e.* 1 SPRYSEC for 3.33 Mb (Mei *et al.* 2015; Eves-van den
481 Akker *et al.* 2016). When looking at the genic environment of outlier loci, we explored a total
482 of 2 Mb of the genome and we identified 15 SPRY domain containing proteins, *i.e.* 1 for 133
483 kb, and 3 SPRYSECs, *i.e.* 1 for 660 kb. This is more than expected by chance in both cases
484 and therefore support the view that some SPRYSEC proteins should be well indeed involved
485 in the adaptation of *G. pallida* to Iledher.

486 It can be noticed that the lnRH test also identified, among the 275 outlier loci, six
487 SNPs showing a decrease of genetic diversity in both Désirée lineages (data not shown).
488 These loci were distributed on four scaffolds, different from those on which the 31 outliers
489 were located. Although we did not consider them in this study, those results could further be
490 used to study adaptation to the potato cultivar Désirée. Only one of the 13 microsatellite
491 markers identified as outliers by Eoche-Bosy *et al.* (2016) was located on the same scaffold as
492 one of the 31 outlier SNPs identified here, and no one was located on the same scaffold as the
493 six outlier SNPs involved in Désirée adaptation. The microsatellite marker Gp235 was indeed
494 located at about 150 bp from the outlier SNP identified here on the scaffold 216. The fact that
495 the other outlier microsatellites were not found on the same scaffold that outlier SNPs is not
496 surprising, due to the small number of microsatellites used and to the fragmentation of the
497 genome.

498 By identifying genomic regions putatively involved in the adaptation to the resistance
499 from *S. vernei*, the present study has taken a further step towards understanding and

500 identifying the determinants of virulence. In the aim of pinpointing, among the candidate loci,
501 those actually involved in the adaptation to the potato cultivar Iledher, a first step of
502 validation could consist of studying allele frequencies of candidate SNPs in natural
503 populations showing different virulence level to Iledher, which could allow to validate some
504 of them whose variations in allelic frequencies would correlate with variations in virulence
505 level. Even if those loci are not the mutation responsible for the adaptation, they can be
506 enough linked to it to be used as molecular tools to determine virulence allele frequencies in
507 field populations before the deployment of resistant cultivars, and to study more accurately
508 the potential fitness costs or benefits linked to the mutation from avirulence to virulence.
509 Indeed, a recent study suggested that adaptation to Iledher involves an increase of fitness on a
510 susceptible potato cultivar (Fournet *et al.* 2016). However, this study did not test for
511 competition between avirulent and virulent individuals, because of the lack of molecular
512 markers allowing to follow (a)virulence alleles. And it was shown in the *Potato Virus Y* that a
513 cost of competitiveness could occur, even in absence of fitness cost in simple inoculation
514 (Janzac *et al.* 2010). The identified outlier loci will also allow to target more precisely the best
515 candidate genes involved in the adaptation, which will have to be functionally validated.

516

517 **Acknowledgments**

518 The authors gratefully acknowledge D. Mugniéry and M.C. Kerlan who took part in the
519 experimental evolution, L. Renault, S. Bardou-Valette, C. Porte and D. Fouville who helped
520 for the protocol elaboration and the pooled samples preparation, and M. Vidal for its help in
521 libraries preparation. DEB is supported by the INRA department SPE and the Région
522 Bretagne through a three year PhD grant.

523 **References**

- 524 Alenda C, Montarry J, Grenier E (2014) Human influence on the dispersal and genetic
525 structure of French *Globodera tabacum* populations. *Infection, Genetics and Evolution*, **27**,
526 309-317.
- 527 Ayme V, Souche S, Caranta C *et al.* (2006) Different mutations in the genome-linked protein
528 VPg of *Potato virus Y* confer virulence on the *pvr2*³ resistance in pepper. *Molecular Plant-*
529 *Microbe Interactions*, **19**, 557-563.
- 530 Barbary A, Djian-Caporalino C, Palloix A, Castagnone-Sereno P (2015) Host genetic
531 resistance to root-knot nematodes, *Meloidogyne* spp., in Solanaceae: from genes to the
532 field. *Pest Management Science*, **71**, 1591–1598.
- 533 Bekal S, Domier LL, Gonfa B, Lakhssassi N, Meksem K, Lambert KN (2015). A SNARE-
534 like protein and biotin are implicated in soybean cyst nematode virulence. *PLoS ONE*, **10**,
535 e0145601.
- 536 Blankenberg D, Von Kuster G, Coraor N *et al.* (2010) Galaxy: a web-based genome analysis
537 tool for experimentalists. *Current Protocols in Molecular Biology*, **89**, 19.10.1-19.10.21.
- 538 Bonhomme M, Chevalet C, Servin B *et al.* (2010) Detecting selection in population trees: the
539 Lewontin and Krakauer test extended. *Genetics*, **186**, 241-262.
- 540 Carpentier J, Esquibet M, Fouville D, Manzanares-Dauleux MJ, Kerlan MC, Grenier E (2012)
541 The evolution of the *Gp-Rbp-1* gene in *Globodera pallida* includes multiple selective
542 replacements. *Molecular Plant Pathology*, **13**, 546-555.
- 543 Castagnone-Sereno P (2002) Genetic variability of nematodes: a threat to the durability of
544 plant resistance genes? *Euphytica*, **124**, 193-199.
- 545 Clément JA, Toulza E, Gautier M *et al.* (2013) Private selective sweeps identified from next-
546 generation pool-sequencing reveal convergent pathways under selection in two inbred
547 *Schistosoma mansoni* strains. *PLoS Neglected Tropical Diseases*, **7**, e2591.
- 548 Coop G, Witonsky D, Rienzo A, Pritchard JK (2010) Using environmental correlations to
549 identify loci underlying local adaptation. *Genetics*, **185**, 1411-1423.
- 550 Cotton JA, Lilley CJ, Jones LM *et al.* (2014) The genome and life-stage specific
551 transcriptomes of *Globodera pallida* elucidate key aspects of plant parasitism by a cyst
552 nematode. *Genome Biology*, **15**, R43.
- 553 Davis EL, Hussey RS, Baum TJ *et al.* (2000) Nematode parasitism genes. *Annual Review of*
554 *Phytopathology*, **38**, 365-396.
- 555 DePristo MA, Banks E, Poplin R *et al.* (2011) A framework for variation discovery and
556 genotyping using next-generation DNA sequencing data. *Nature Genetics*, **43**, 491-498.
- 557 Díaz JA, Nieto C, Moriones E, Truniger V, Aranda MA (2004) Molecular characterization of
558 a *Melon necrotic spot virus* strain that overcomes the resistance in melon and nonhost
559 plants. *Molecular Plant-Microbe Interactions*, **17**, 668-675.
- 560 Diaz-Granados A, Petrescu AJ, Goverse A, Smant G (2016) SPRYSEC effectors: a versatile
561 protein-binding platform to disrupt plant innate immunity. *Frontiers in Plant Science*, **7**,
562 1575.
- 563 Djian-Caporalino C, Palloix A, Fazari A *et al.* (2014) Pyramiding, alternating or mixing:
564 comparative performances of deployment strategies of nematode resistance genes to
565 promote plant resistance efficiency and durability. *BMC Plant Biology*, **14**, 53.
- 566 Endo BY (1987) Ultrastructure of esophageal gland secretory granules in juveniles of
567 *Heterodera glycines*. *Journal of Nematology*, **19**, 469-483.
- 568 Eoche-Bosy D, Gauthier J, Juhel AS *et al.* (2016). Experimentally evolved populations of the
569 potato cyst nematode *Globodera pallida* allow the targeting of genomic footprints of
570 selection due to host adaptation. *Plant Pathology*, doi: 10.1111/ppa.12646.

571 Eves-van den Akker S, Birch PR (2016) Opening the effector protein toolbox for plant-
572 parasitic cyst-nematode interactions. *Molecular Plant*, **9**, 1451-1453.

573 Eves-van den Akker S, Laetsch DR, Thorpe P *et al.* (2016) The genome of the yellow potato
574 cyst nematode, *Globodera rostochiensis*, reveals insights into the basis of parasitism and
575 virulence. *Genome Biology*, **17**, 124.

576 Ferretti L, Ramos-Onsins SE, Pérez-Enciso M (2013) Population genomics from pool
577 sequencing. *Molecular Ecology*, **22**, 5561-5576.

578 Fischer MC, Rellstab C, Tedder A *et al.* (2013) Population genomic footprints of selection
579 and associations with climate in natural populations of *Arabidopsis halleri* from the Alps.
580 *Molecular Ecology*, **22**, 5594-5607.

581 Förstner W, Moonen B (2003) A metric for covariance matrices. In: *Geodesy-The Challenge*
582 *of the 3rd Millennium* (eds Grafarend EW, Krumm FW, Schwarze VS), pp. 299-309.
583 Springer-Verlag, Berlin/Heidelberg, Germany.

584 Fournet S, Eoche-Bosy D, Renault L, Hamelin FM, Montarry J (2016) Adaptation to resistant
585 hosts increases fitness on susceptible hosts in the plant parasitic nematode *Globodera*
586 *pallida*. *Ecology and Evolution*, **6**, 2559-2568.

587 Fournet S, Kerlan MC, Renault L, Dantec JP, Rouaux C, Montarry J (2013) Selection of
588 nematodes by resistant plants has implications for local adaptation and cross-virulence.
589 *Plant Pathology*, **62**, 184-193.

590 Futschik A, Schlötterer C (2010) The next generation of molecular markers from massively
591 parallel sequencing of pooled DNA samples. *Genetics*, **186**, 207-218.

592 Gautier M (2015) Genome-wide scan for adaptive differentiation and association analysis
593 with population-specific covariables. *Genetics*, **201**, 1555-1579.

594 Gautier M, Foucaud J, Gharbi K *et al.* (2013) Estimation of population allele frequencies
595 from next-generation sequencing data: pool-versus individual-based genotyping.
596 *Molecular Ecology*, **22**, 3766-3779.

597 Green CD, Greet DN, Jones FGW (1970) The influence of multiple mating on the
598 reproduction and genetics of *Heterodera rostochiensis* and *H. schachtii*. *Nematologica*, **16**,
599 309-326.

600 Günther T, Coop G (2013) Robust identification of local adaptation from allele frequencies.
601 *Genetics*, **195**, 205-220.

602 Haegeman A, Mantelin S, Jones JT, Gheysen G (2012) Functional roles of effectors of plant-
603 parasitic nematodes. *Gene*, **492**, 19-31.

604 Janzac B, Fabre F, Palloix A, Moury B (2009) Constraints on evolution of virus avirulence
605 factors predict the durability of corresponding plant resistances. *Molecular Plant*
606 *Pathology*, **10**, 599-610.

607 Janzac B, Montarry J, Palloix A, Navaud O, Moury B (2010) A point mutation in the
608 polymerase *Potato Virus Y* confers virulence toward the *Pvr4* resistance of pepper and a
609 high competitiveness cost in susceptible cultivar. *Molecular Plant-Microbe Interactions*,
610 **23**, 823-830.

611 Jeffreys H (1961) *Theory of Probability*, 3rd edn. Oxford University Press, Oxford, UK.

612 Jones FGW (1950) Observations on the beet eelworm and other cyst-forming species of
613 *Heterodera*. *Annals of Applied Biology*, **37**, 407-440.

614 Jones MGK, Northcote DH (1972) Nematode-induced syncytium – a multinucleate transfer
615 cell. *Journal of Cell Science*, **10**, 789-809.

616 Kauer MO, Dieringer D, Schlötterer C (2003) A microsatellite variability screen for positive
617 selection associated with the “Out of Africa” habitat expansion of *Drosophila*
618 *melanogaster*. *Genetics*, **165**, 1137-1148.

619 Kofler R, Nolte V, Schlötterer C (2016) The impact of library preparation protocols on the
620 consistency of allele frequency estimates in Pool-Seq data. *Molecular Ecology Resources*,
621 **16**, 118-122.

622 Langmead B, Salzberg SL (2012) Fast gapped-read alignment with Bowtie 2. *Nature*
623 *Methods*, **9**, 357-359.

624 Langmead B, Trapnell Cole, Pop M, Salzberg SL (2009) Ultrafast and memory-efficient
625 alignment of short DNA sequences to the human genome. *Genome Biology*, **10**, R25.

626 Li H, Handsaker B, Wysoker A *et al.* (2009) The Sequence Alignment/Map format and
627 SAMtools. *Bioinformatics*, **25**, 2078-2079.

628 Lozano-Torres JL, Wilbers RH, Gawronski P *et al.* (2012) Dual disease resistance mediated
629 by the immune receptor Cf-2 in tomato requires a common virulence target of a fungus and
630 a nematode. *Proceedings of the National Academy of Sciences of the United States of*
631 *America*, **109**, 10119-10124.

632 Lozano-Torres JL, Wilbers RH, Warmerdam S *et al.* (2014) Apoplastic venom allergen-like
633 proteins of cyst nematodes modulate the activation of basal plant innate immunity by cell
634 surface receptors. *PLoS Pathogens*, **10**, e1004569.

635 Luikart G, England PR, Tallmon D, Jordan S, Taberlet P (2003) The power and promise of
636 population genomics: from genotyping to genome typing. *Nature Reviews Genetics*, **4**,
637 981-994.

638 Mardis ER (2008) The impact of next-generation sequencing technology on genetics. *Trends*
639 *in Genetics*, **24**, 133-141.

640 McDonald BA, Linde C (2002) Pathogen population genetics, evolutionary potential, and
641 durable resistance. *Annual Review of Phytopathology*, **40**, 349-379.

642 McEvoy B, Beleza S, Shriver MD (2006) The genetic architecture of normal variation in
643 human pigmentation: an evolutionary perspective and model. *Human Molecular Genetics*,
644 **15**, R176-R181.

645 McKenna A, Hanna M, Banks E *et al.* (2010) The Genome Analysis Toolkit: A MapReduce
646 framework for analyzing next-generation DNA sequencing data. *Genome Research*, **20**,
647 1297-1303.

648 Mei Y, Thorpe P, Guzha A *et al.* (2015) Only a small subset of the SPRY domain gene family
649 in *Globodera pallida* is likely to encode effectors, two of which suppress host defences
650 induced by the potato resistance gene *Gpa2*. *Nematology*, **17**, 409-424.

651 Meshi T, Motoyoshi F, Adachi A, Watanabe Y, Takamatsu N, Okada Y (1988) Two
652 concomitant base substitutions in the putative replicase genes of tobacco mosaic virus
653 confer the ability to overcome the effects of a tomato resistance gene, *Tm-1*. *EMBO*
654 *Journal*, **7**, 1575-1581.

655 Mitchum MG, Hussey RS, Baum TJ *et al.* (2013) Nematode effector proteins: an emerging
656 paradigm of parasitism. *New Phytologist*, **199**, 879-894.

657 Montarry J, Jan PL, Gracianne C *et al.* (2015) Heterozygote deficits in cyst plant-parasitic
658 nematodes: possible causes and consequences. *Molecular Ecology*, **24**, 1654-1677.

659 Nicol JM, Turner SJ, Coyne DL, den Nijs L, Hockland S, Maafi ZT (2011) Current nematode
660 threats to world agriculture. In: *Genomics and Molecular Genetics of Plant-Nematode*
661 *Interactions* (eds Jones J, Gheysen G, Fenoll C), pp. 21-43. Springer, Dordrecht, The
662 Netherlands.

663 Oerke EC, Dehne HW, Schönbeck F, Weber A (1994) *Crop production and crop protection:*
664 *estimated losses in major food and cash crop*. Elsevier Science BV, Amsterdam, The
665 Netherlands.

666 Parra G, Bradnam K, Korf I (2007) CEGMA: A pipeline to accurately annotate core genes in
667 eukaryotic genomes. *Bioinformatics*, **23**, 1061-1067.

668 Pavlidis P, Jensen JD, Stephan W, Stamatakis A (2012) A critical assessment of storytelling:
669 gene ontology categories and the importance of validating genomic scans. *Molecular*
670 *Biology and Evolution*, **29**, 3237-3248.

671 Petersen TN, Brunak S, von Heijne G, Nielsen H (2011) SIGNALP 4.0: discriminating signal
672 peptides from transmembrane regions. *Nature Methods*, **8**, 785-786.

673 Picard D, Plantard O, Scurrah M, Mugniéry D (2004) Inbreeding and population structure of
674 the potato cyst nematode (*Globodera pallida*) in its native area (Peru). *Molecular Ecology*,
675 **13**, 2899-2908.

676 Plantard O, Porte C (2004) Population genetic structure of the sugar beet cyst nematode
677 *Heterodera schachtii*: a gonochoristic and amphimictic species with highly inbred but
678 weakly differentiated populations. *Molecular Ecology*, **13**, 33-41.

679 Rehman S, Postma W, Tytgat T *et al.* (2009) A secreted SPRY domain-containing protein
680 (SPRYSEC) from the plant-parasitic nematode *Globodera rostochiensis* interacts with a
681 CC-NB-LRR protein from a susceptible tomato. *Molecular Plant-Microbe Interactions*,
682 **22**, 330-340.

683 Rellstab C, Zoller S, Tedder A, Gugerli F, Fischer MC (2013) Validation of SNP allele
684 frequencies determined by pooled next-generation sequencing in natural populations of a
685 non-model plant species. *PLoS ONE*, **8**, e80422.

686 Rhodes J, Beale MA, Fisher MC (2014) Illuminating choices for library prep: a comparison of
687 library preparation methods for whole genome sequencing of *Cryptococcus neoformans*
688 using Illumina HiSeq. *PLoS One*, **9**, e113501.

689 Rouppe van der Voort JNAM, van der Vossen E, Bakker E *et al.* (2000) Two additive QTLs
690 conferring broad-spectrum resistance in potato to *Globodera pallida* are localized on
691 resistance gene clusters. *Theoretical and Applied Genetics*, **96**, 654-661.

692 Rouppe van der Voort JNAM, van Eck HJ, van Zandvoort PM, Overmars H, Helder J, Bakker
693 J (1999) Linkage analysis by genotyping of sibling populations: a genetic map for the
694 potato cyst nematode constructed using a 'pseudo-F2' mapping strategy. *Molecular and*
695 *General Genetics*, **261**, 1021-31.

696 Rubin CJ, Megens HJ, Barrio AM *et al.* (2012) Strong signatures of selection in the domestic
697 pig genome. *Proceedings of the National Academy of Sciences of the United States of*
698 *America*, **109**, 19529-19536.

699 Rubin CJ, Zody MC, Eriksson J *et al.* (2010) Whole-genome resequencing reveals loci under
700 selection during chicken domestication. *Nature*, **464**, 587-591.

701 Sacco MA, Koropacka K, Grenier E *et al.* (2009) The cyst nematode SPRYSEC protein RBP-
702 1 elicits Gpa2- and RanGAP2-dependent plant cell death. *PLoS Pathogens*, **5**, e1000564.

703 Schlötterer C, Dieringer D (2005) A novel test statistic for the identification of local selective
704 sweeps based on microsatellite gene diversity. In: *Selective Sweep* (ed. Nurminsky D), pp.
705 55-64. Landes Bioscience, Georgetown, USA.

706 Schlötterer C, Tobler R, Kofler R, Nolte V (2014) Sequencing pools of individuals – mining
707 genome-wide polymorphism data without big funding. *Nature Review Genetics*, **15**, 749-
708 763.

709 Sobczak M, Golinowski W (2011) Cyst nematodes and syncytia. In: *Genomics and molecular*
710 *genetics of plant-nematode interactions* (eds Jones JT, Gheysen G, Fenoi C), pp. 61-82.
711 Springer, Dordrecht, The Netherlands.

712 Storz JF (2005) Using genome scans of DNA polymorphism to infer adaptive population
713 divergence. *Molecular Ecology*, **14**, 671-688.

714 Triantaphyllou AC, Esbenshade PR (1990) Demonstration of multiple mating in *Heterodera*
715 *glycines* with biochemical markers. *Journal of Nematology*, **22**, 452-456.
716 Van der Auwera GA, Carneiro MO, Hartl C *et al.* (2013) From FastQ data to high confidence
717 variant calls: the Genome Analysis Toolkit best practices pipeline. *Current Protocols in*
718 *Bioinformatics*, **43**, 11.10.1-11.10.33.
719 van Riel HR, Mulder A (1998) Potato cyst nematodes (*Globodera* species) in western Europe.
720 In: *Potato Cyst Nematodes: Biology, Distribution and Control* (eds Marks RJ, Brodie BB),
721 pp. 271-298. CAB International, Wallingford, UK.
722 Vasemägi A, Nilsson J, McGinnity P *et al.* (2012) Screen for footprints of selection during
723 domestication/captive breeding of Atlantic Salmon. *Comparative and Functional*
724 *Genomics*, **2012**, 628204.
725 von Mende N (1997) Invasion and migration behaviour of sedentary nematodes. In: *Cellular*
726 *and Molecular Aspects of Plant–Nematodes Interactions* (eds Fenoll C, Grundler FMW,
727 Ohl SA), pp. 51-64. Kluwer Academic Publishers, Dordrecht, The Netherlands.
728 Zhu Y, Bergland AO, González J, Petrov DA (2012) Empirical validation of pooled whole
729 genome population re-sequencing in *Drosophila melanogaster*. *PLoS One*, **7**, e41901.
730

731 **Data accessibility**

732 Sequencing data were submitted to the BBRIC Archive network ([https://bbric-](https://bbric-archive.toulouse.inra.fr/web/index.html)
733 [archive.toulouse.inra.fr/web/index.html](https://bbric-archive.toulouse.inra.fr/web/index.html)) in Project Gpool.

734

735 **Author Contributions**

736 SF performed the experimental evolution. DEB, ME, SF and JM performed the experiments
737 according to a protocol elaborated jointly by DEB, EG and JM. OB performed the Illumina
738 sequencing at the GeT-PlaGe platform (Toulouse, France). DEB, MG, FL and AB analyzed
739 the data. DEB and JM wrote the text and prepared the figures. All authors edited the article
740 and have approved the current version.

741

742 **Supporting information**

743 Additional supporting information may be found on the online version of this article.

744 **Figure S1** Principal Component Analysis (PCA) of the sequencing data from eight *G. pallida*
745 pools sequenced on four lanes (technical replicates), based on read counts at 2,383,040 SNPs.

746 **Table S2** Putative functions of the predicted genes located in a 120-kb window centered on
747 the 31 outlier loci on the *Globodera pallida* genome assembly version Gpal.v1.0 (Cotton *et*
748 *al.* 2014).

749 **Figure legends**

750

751 **Fig. 1** Selection of the four experimental *Globodera pallida* lineages. Nematode lineages
752 were established from two French natural *G. pallida* populations, SM (near Saint-Malo,
753 Brittany, north-western France) and N (from the island of Noirmoutier, western France),
754 reared during eight successive cycles (*i.e.* eight generations) on the susceptible potato cultivar
755 Désirée (D) and on the resistant cultivar Iledher (I). Each sample name indicates its
756 geographical origin (SM for Saint-Malo and N for Noirmoutier) and the potato cultivar on
757 which it evolved (I for Iledher and D for Désirée).

758

759 **Fig. 2** Inferred relationship among the eight *G. pallida* lineages represented by a correlation
760 plot and a hierarchical clustering tree derived from the matrix Ω estimated under the core
761 model. Each sample name indicates its geographical origin (SM for Saint-Malo and N for
762 Noirmoutier), the potato cultivar on which it evolved (I for Iledher and D for Désirée) and the
763 replicate number (1 or 2).

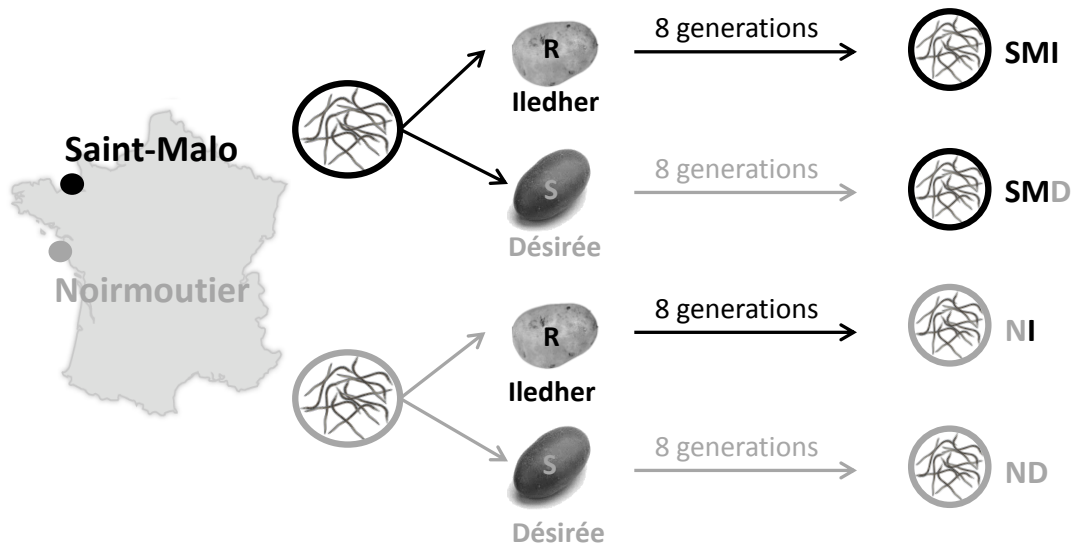
764

765 **Fig. 3** SNP XtX as a function of the BF_{mc} for association with the virulence status covariable,
766 estimated in one of the three independent analyses. The vertical dotted line represents the 1%
767 POD significance threshold ($XtX = 14.0$) and the horizontal dotted line represents the 20 dB
768 threshold for BF_{mc} . Black dots represent the 275 outlier loci of interest (*i.e.* outliers for both
769 XtX and BF_{mc} values) and red dots represent the 31 outlier loci of strong interest (*i.e.* outliers
770 also identified with lnRH).

771

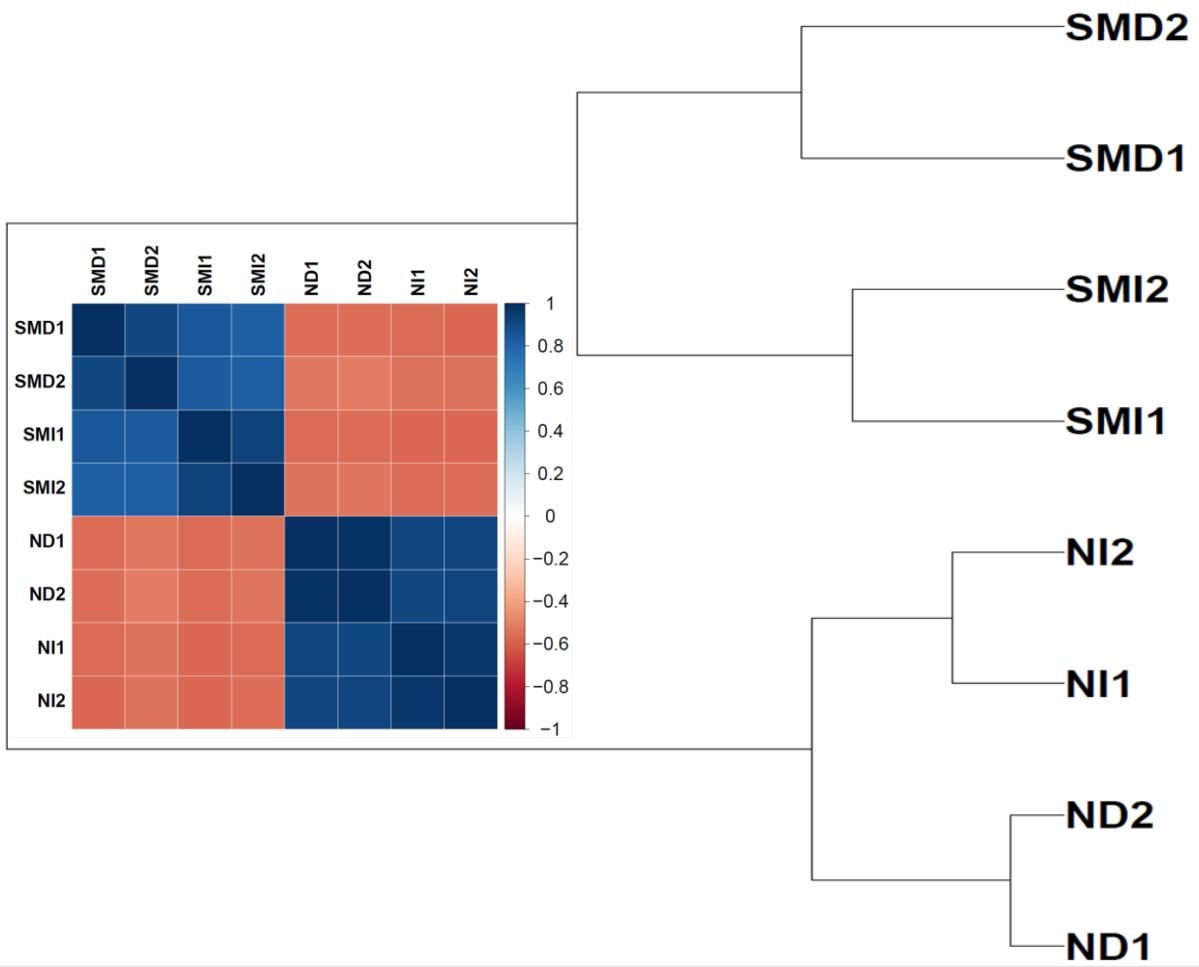
772 **Fig. 4** Example of increase of genetic differentiation (represented as XtX estimates computed
773 in BayPass across the whole dataset) and decrease of genetic diversity (represented as
774 expected heterozygosity H in each lineages having evolved on Iledher) in a candidate
775 genomic region. The scaffold represented is the scaffold 988 and the grey line indicates the
776 location of the four outlier SNPs on the scaffold.

777 **Figure 1 – Eoche-Bosy et al.**



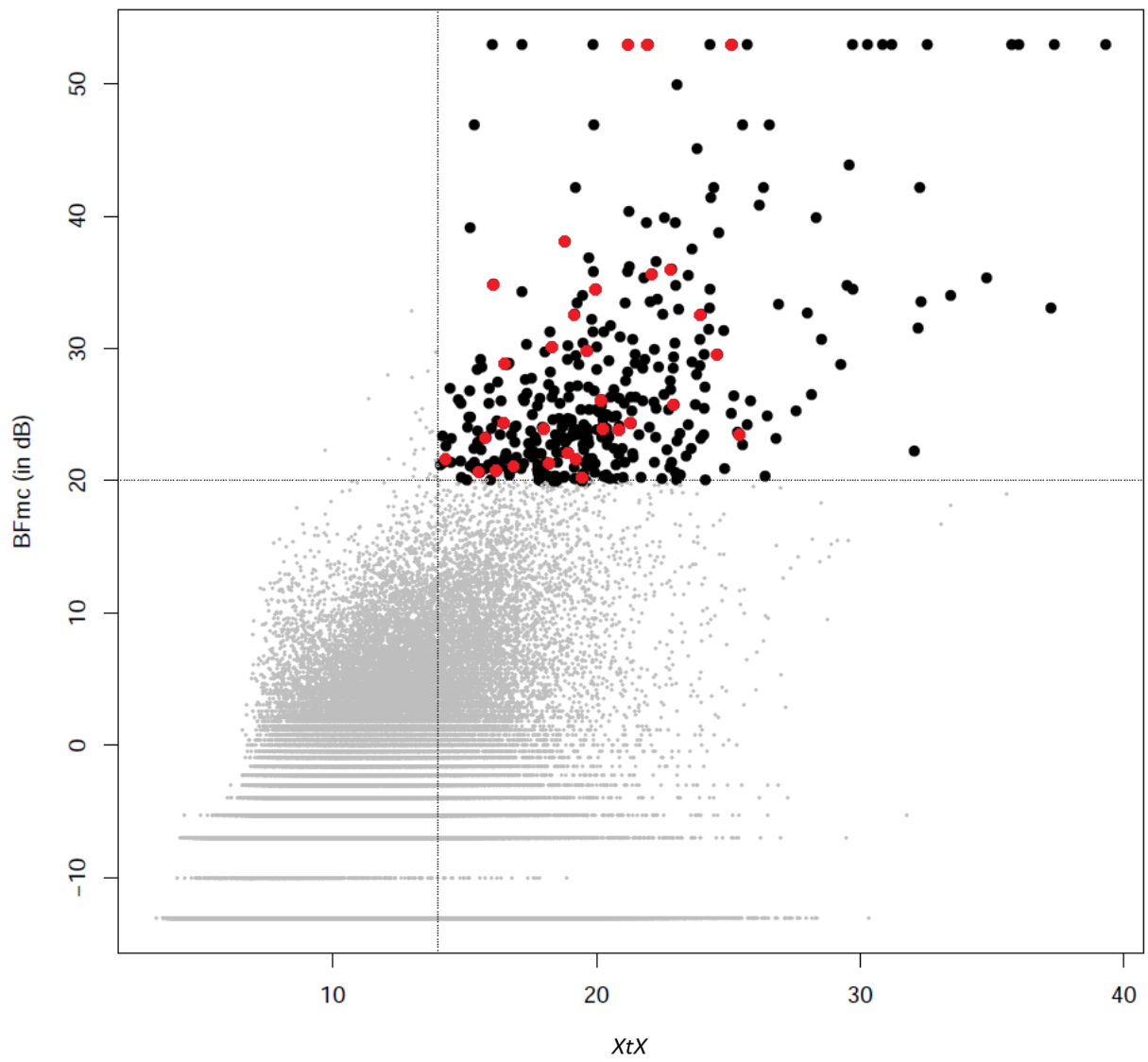
778

779 **Figure 2 – Eoche-Bosy et al.**



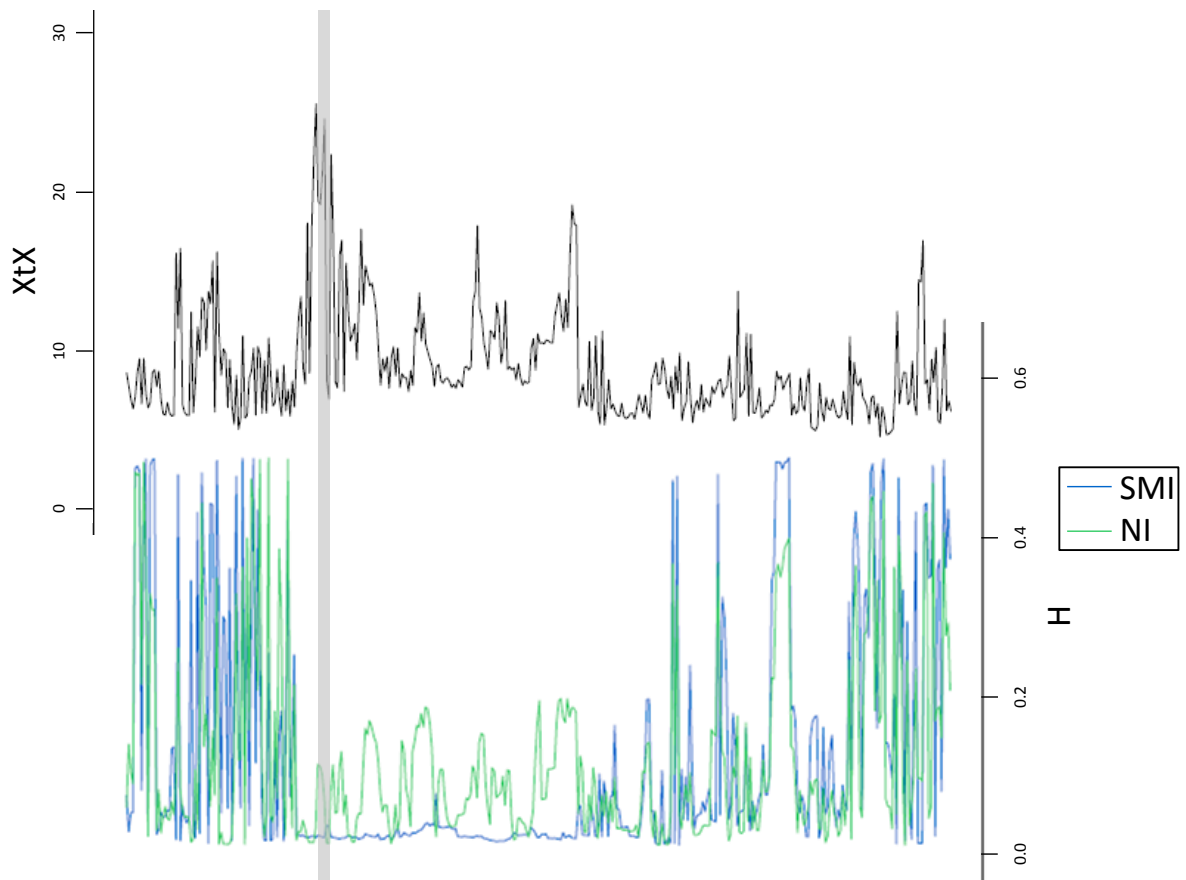
780

781 **Figure 3 – Eoche-Bosy et al.**



782

783 **Figure 4 – Eoche-Bosy et al.**



784

785 **Supporting Information**

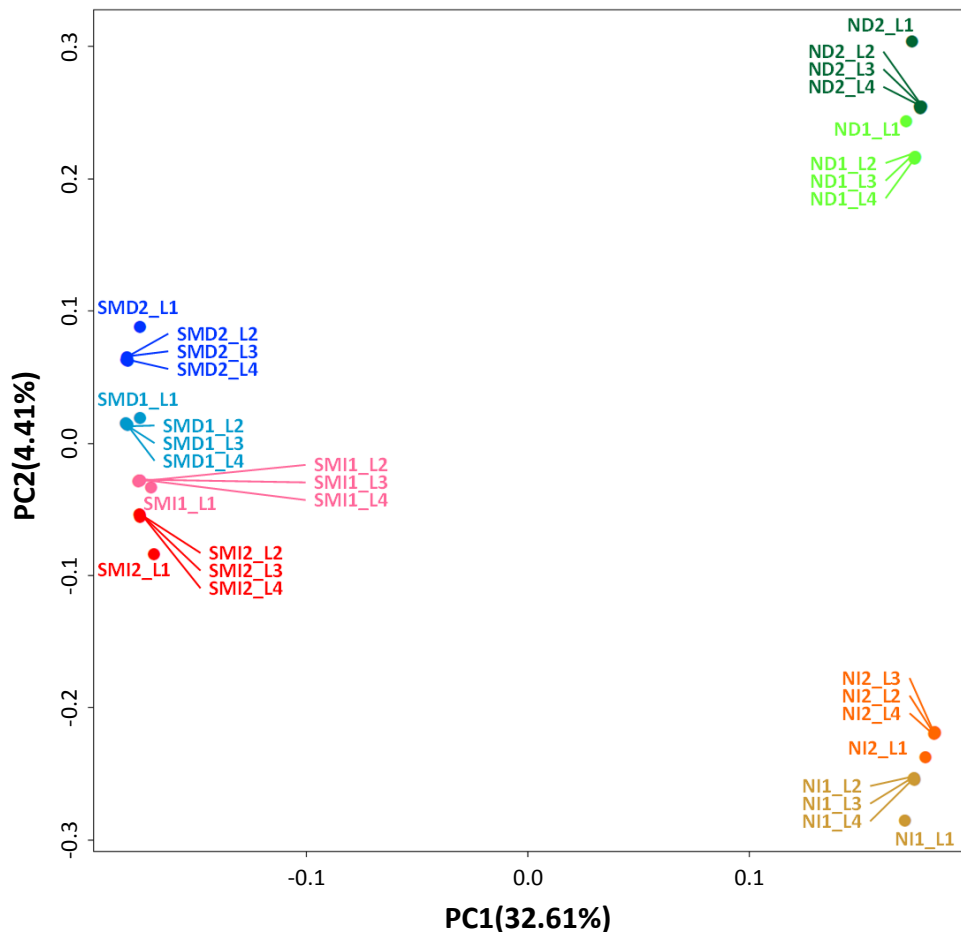
786 **Supplementary Figure S1**

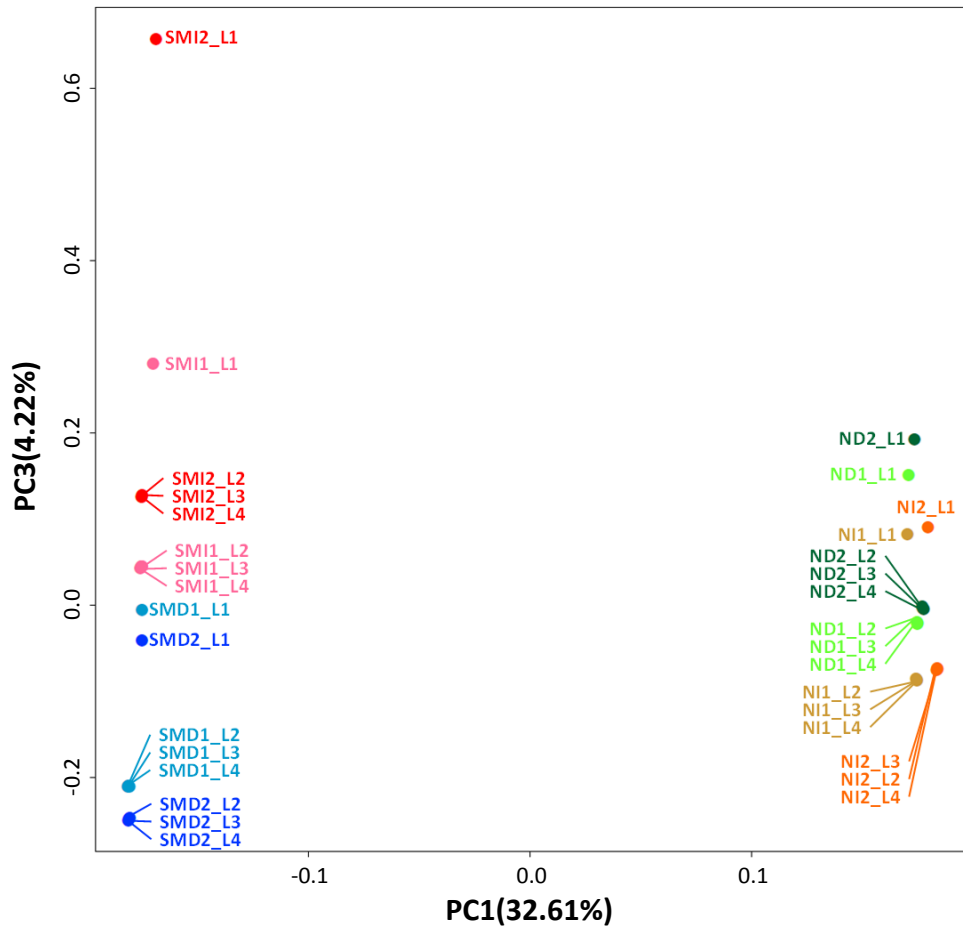
787 Principal Component Analysis (PCA) of the sequencing data from eight *G. pallida* pools
788 sequenced on four different lanes (technical replicates), based on read counts at 2,383,040
789 SNPs. Each sample name indicates its geographical origin (SM for Saint-Malo and N for
790 Noirmoutier), the potato cultivar on which it evolved (I for Iledher and D for Désirée), the
791 number of the biological replicate (1 or 2) and the number of the lane (L) on which it has been
792 sequenced. The first axis explains 32.61% of the variance and clusters the samples according
793 to the population geographical origin. Even if the second and third axes explain a small part
794 of the variance, *i.e.* 4.41% for PC2 and 4.22% for PCA3, they tend to cluster N and SM
795 samples, respectively, according to their virulence status. Note however that for each of the
796 eight pools, replicate sequenced on the first sequencing lane systematically depart from the
797 three others. This patterns most probably results from a lower sequencing coverage for lane 1
798 (that was sequenced in 2x100 bp paired end) compared to the three others (that were
799 sequenced in 2x125 bp paired-end)

800

801

802





804 **Supplementary Table S2**

805 Putative functions of the predicted genes located in a 120-kb window centered on the 31 outlier loci on the *Globodera pallida* genome
 806 assembly version Gpal.v1.0 (Cotton *et al.* 2014). Relevant results of the BLAST search of the predicted genes against the annotated *G.*
 807 *rostochiensis* genome version nGr.v1.0 (Eves-van den Akker *et al.* 2016) are also shown. *: outlier SNP located in the gene, **: outlier
 808 SNP located in the exon.

809
 810

Scaffold	Outlier locus	<i>Globodera pallida</i> genome				BLAST against <i>Globodera rostochiensis</i> genome	
		Gene ID	Location on the scaffold	Putative gene function	Peptide signal	Gene ID	Putative gene function
4	SNP_4_429075	GPLIN_000030900	367074-371195	actin protein 6	no	GROS_g12208	spliceosome
		GPLIN_000031000	371242-372608	nuclear Pore complex protein family member	no		
		GPLIN_000031100	398790-400048	transcription initiation factor TFIID subunit	no		
		GPLIN_000031200	403834-404255	beta 1 4 endoglucanase	no		
		GPLIN_000031300*	428992-438734	transcribed hypothetical protein	no	GROS_g05341	magnesium ion transport; sodium ion transmembrane transport; integral to plasma membrane; cation channel activity
		GPLIN_000031400	439019-440137	transcribed hypothetical protein	no		
		GPLIN_000031500	441856-451123	cysteine synthase	no		
		GPLIN_000031600	457740-458980	long chain fatty acid transport protein 4	no	GROS_g13363	fatty acid transport proteins
		GPLIN_000031700	460388-460633	transcribed hypothetical protein	no		
		GPLIN_000031800	462978-464011	beta 1,3 galactosyltransferase 2	no	GROS_g00450	galactosyltransferase
		GPLIN_000031900	470256-470486	transcribed hypothetical protein	no		
		GPLIN_000032000	471353-473130	transcribed hypothetical protein	no		
		GPLIN_000032100	474046-474331	transcribed hypothetical protein	no	GROS_g10714	protein binding; stress-activated map kinase interacting protein 1 (SIN1)

	GPLIN_0001 49900	243326-245017	solute carrier family 35 member B1	yes	GROS_g0215 1	transport
	GPLIN_0001 50000	245308-249627	mitogen activated protein kinase kinase kinase	no	GROS_g0215 0	MAPK signaling pathway
	GPLIN_0001 50100	251276-252209	superoxide dismutase (Cu Zn)	yes	GROS_g0214 9	peroxisome
	GPLIN_0001 50200	252398-253488	transcribed hypothetical protein	no	GROS_g0214 8	transmembrane
	GPLIN_0001 50300	254217-258092	transcribed hypothetical protein	no	GROS_g0214 6	RNA transport; negative regulation of DNA damage checkpoint
	GPLIN_0001 50400	258929-261360	T complex protein 1 subunit epsilon	no	GROS_g0214 5	cytoskeleton organization; posttranslational protein folding
	GPLIN_0001 50500	261650-263494	transcribed hypothetical protein	no	GROS_g1428 2	metabolism of xenobiotics by cytochrome P450
	GPLIN_0001 50600	263679-265256	protein vertebrate galectins	yes	GROS_g0214 3	galactose binding; signal transducer activity
	GPLIN_0001 50700	265891-266885	N alpha acetyltransferase 20	no	GROS_g0214 1	endocytosis
	GPLIN_0001 50800	266955-269813	transcribed hypothetical protein	no	GROS_g0214 0	protein homodimerization activity
	SNP_25_304232 GPLIN_0001 50900	269952-271262	transcribed hypothetical protein	no	GROS_g0213 9	transmembrane
	GPLIN_0001 51000	271403-272406	transcribed hypothetical protein	no		
	GPLIN_0001 51100	273509-275230	fasciculation and elongation protein zeta 2	no	GROS_g0213 7	axon guidance
	GPLIN_0001 51200	275973-277291	protein kinase domain containing protein, ck worm protein kinase	no		
	GPLIN_0001 51300	279494-280946	calmodulin	no	GROS_g0213 6	calmodulin
	GPLIN_0001 51400	284171-284443	transcribed hypothetical protein	no		
	GPLIN_0001 51500	299966-302277	cyclin-dependent kinase inhibitor	no		
	GPLIN_0001 51600*	303454-310418	exportin 7	no	GROS_g0213 1	nuclear export signal receptor activity; protein export from nucleus; nuclear pore
	GPLIN_0001 51700	310648-311820	glutaredoxin 3	no	GROS_g0213 0	glutaredoxin-3
	GPLIN_0001 51800	313085-314369	transcribed hypothetical protein	no		
	GPLIN_0001 51900	315934-316953	transcribed hypothetical protein	no	GROS_g0212 9	transmembrane
	GPLIN_0001 52000	317223-324014	DEAD Box protein	no	GROS_g0212 8	ATP catabolic process

	GPLIN_0001 52100	328566-329000	transcribed hypothetical protein	no		
	GPLIN_0001 52200	329118-330907	transcribed hypothetical protein	no	GROS_g0212 6	chromatin binding
	GPLIN_0001 52300	335501-336396	immunoglobulin i set domain containing protein	yes	GROS_g0212 5	transmembrane
	GPLIN_0001 52400	336805-340764	transcribed hypothetical protein	no	GROS_g0212 4	Golgi apparatus
	GPLIN_0001 52500	341193-341716	transcribed hypothetical protein	no		
<hr/>						
	GPLIN_0002 32300	163392-163732	transcribed hypothetical protein	no		
	GPLIN_0002 32400	168518-169562	transcribed hypothetical protein	yes	GROS_g0408 5	signal peptide
	GPLIN_0002 32500	169991-170378	transcribed hypothetical protein	no		
	GPLIN_0002 32600	171849-174837	transcribed hypothetical protein	yes	GROS_g0408 7	signal peptide
	GPLIN_0002 32700	180474-181761	phosphatidylcholine:ceramide	no	GROS_g0408 9	sphingolipid metabolism
	GPLIN_0002 32800	183265-184828	60S ribosomal protein L4	no	GROS_g0409 0	cell wall modification; ribosomal protein L1e signature
	GPLIN_0002 32900	184937-188002	palmitoyltransferase ZDHHC2	no	GROS_g0409 1	proteinS-acyltransferase
	GPLIN_0002 33000	196131-198830	transcribed hypothetical protein	no	GROS_g1153 9	Transmembrane
	GPLIN_0002 33100	198931-200169	transcribed hypothetical protein	no		
	GPLIN_0002 33200	200212-201447	transcribed hypothetical protein	no		
SNP_44_221212	GPLIN_0002 33300	201499-202356	transcribed hypothetical protein	no		
44	GPLIN_0002 33400	202494-203706	transcribed hypothetical protein	no		
SNP_44_221214	GPLIN_0002 33500	203859-205030	worm specific Argonaute NRDE 3	no		
	GPLIN_0002 33600	205120-205935	transcription factor TFIIID, C-terminal DNA glycosylase, N-terminal	no		
	GPLIN_0002 33700	206066-211386	transcribed hypothetical protein	no		
	GPLIN_0002 33800	211708-212533	transcribed hypothetical protein	no		
	GPLIN_0002 33900	212735-214448	transcribed hypothetical protein	no		

	GPLIN_0002 34000	221431-221718	transcribed hypothetical protein	no		
	GPLIN_0002 34100	221849-222821	polynucleotide kinase 3' phosphatase	no		
	GPLIN_0002 34200	255627-261288	macrophage erythroblast attacher	yes	GROS_g0323 9	CTLH/CRA C-terminal to LisH motif domain; actin cytoskeleton; negative regulation of myeloid cell apoptotic process
	GPLIN_0002 34300	264876-267441	mitochondrial processing peptidase beta subunit	no	GROS_g0323 5	insulinase (peptidase family M16)
	GPLIN_0002 34400	268640-269749	U1 small nuclear ribonucleoprotein A	no	GROS_g0323 4	regulation of alternative nuclear mRNA splicing, via spliceosome
	GPLIN_0002 34500	270323-271985	guanine nucleotide binding protein subunit	no	GROS_g0323 3	small ribosomal subunit; ion channel inhibitor activity
	GPLIN_0002 34600	272436-274181	transcribed hypothetical protein	no	GROS_g0323 2 / GROS_g0323 8	mitochondrion; negative regulation of synaptic transmission, glutamatergic / ATP catabolic process; adenosinetriphosphatase
	GPLIN_0002 34700	274837-276164	receptor expression enhancing protein 5	no	GROS_g0323 1	protein binding
	GPLIN_0002 34800	276256-277074	G protein coupled receptor associated sorting	no		
	GPLIN_0002 34900	277860-282940	4 aminobutyrate aminotransferase, mitochondrial	no	GROS_g0323 0 / GROS_g0323 0	beta-Alanine metabolism / beta-Alanine metabolism
	GPLIN_0003 11400	1-3999	transcribed hypothetical protein	no	GROS_g1278 4	signal peptide
	GPLIN_0003 11500	19418-20911	transcribed hypothetical protein	no	GROS_g1426 0	RBP-4 protein [<i>G. pallida</i>]
	GPLIN_0003 11600	30359-32404	transcribed hypothetical protein	no	GROS_g1419 6	RBP-4 protein [<i>G. pallida</i>]; secreted SPRY domain-containing protein 18 [<i>G. rostochiensis</i>]
SNP_66_55507	GPLIN_0003 11700	36477-37252	transcribed hypothetical protein	no		
	GPLIN_0003 11800	45302-45915	transcribed hypothetical protein	no	GROS_g0402 3	riboflavin metabolism
66	SNP_66_131126	46907-48176	BTB:POZ domain containing protein 3	yes	GROS_g1412 8	RBP-1 protein, partial [<i>G. pallida</i>]
	GPLIN_0003 12000	49696-50448	transcribed hypothetical protein	no	GROS_g1413 6	RBP-4 protein [<i>G. pallida</i>]; transmembrane
	GPLIN_0003 12100	53144-55475	protein containing SPRY domain	no	GROS_g1427 8	RBP-1 protein [<i>G. pallida</i>]
	GPLIN_0003 12200	57585-58590	transcribed hypothetical protein	no	GROS_g1118 9	peptidase family M41
	GPLIN_0003 12300	66233-69356	protein containing SPRY domain	no	GROS_g1413 0	truncated secreted SPRY domain-containing protein 15, partial [<i>G. rostochiensis</i>]; signal peptide

	GPLIN_0003 12400	71724-72660	transcribed hypothetical protein	no			
	GPLIN_0003 12500	92978-94740	protein containing SPRY domain	no	GROS_g1427 8	RBP-1 protein [<i>G. pallida</i>]	
	GPLIN_0003 12600	95754-96913	protein containing SPRY domain	no	GROS_g1428 7	truncated secreted SPRY domain-containing protein 15, partial [<i>G. rostochiensis</i>]	
	GPLIN_0003 12700	107749-107949	EF-hand 2 domain containing protein	no	GROS_g1428 1	EF-hand calcium-binding domain.	
	GPLIN_0003 12800	111831-112806	transcribed hypothetical protein	no	GROS_g0572 9	protein SAX-7 ; transmembrane	
	GPLIN_0003 12900	112920-115358	group 1 glycosyl transferase	no	GROS_g0172 7	glycosyl transferases group 1	
	GPLIN_0003 13000	119091-120888	transcribed hypothetical protein	no			
	GPLIN_0003 13100	124022-124830	transcribed hypothetical protein	no			
	GPLIN_0003 13200*	129063-137156	Sensory AXon guidance family member (sax 7)	no	GROS_g0572 9	protein SAX-7; sensory AXon guidance ; transmembrane	
	(SNP_66_13 1126)						
	GPLIN_0003 13300	139135-140624	transcribed hypothetical protein	no			
	GPLIN_0003 13400	142713-144269	transcribed hypothetical protein	no			
	GPLIN_0003 13500	145772-146732	transcribed hypothetical protein	no	GROS_g1327 6	signal peptide	
	GPLIN_0003 13600	154523-157608	beta 1,4 endoglucanase (cell wall modifying protein); putative GH5 cellulase (cellulose degradation)	yes	GROS_g0744 6	beta-1,4-endoglucanase, partial; cellulase	
	GPLIN_0003 13700	158653-160495	transcribed hypothetical protein	no	GROS_g0210 5	poly(A) polymerase central domain; nuclear mRNA splicing, via spliceosome	
	GPLIN_0003 13800	167056-168124	transcribed hypothetical protein	no	GROS_g0744 7	EB module	
	GPLIN_0003 13900	168962-169322	transcribed hypothetical protein	no	GROS_g0112 6	transmembrane	
	GPLIN_0003 14000	183685-184563	transcribed hypothetical protein, similar to <i>G. rostochiensis</i> effector 1106	yes	GROS_g1430 9	signal peptide; 1106 effector family [<i>G. rostochiensis</i>]	
	SNP_85_126066	GPLIN_0003 82000	67804-68769	glutaminyl peptide cyclotransferase	no	GROS_g0737 4	signal peptide; peptidase M28 domain containing protein [<i>Haemonchus contortus</i>]
85		GPLIN_0003 82100	84608-86814	transcribed hypothetical protein	no	GROS_g1412 4	RBP-4 protein [<i>G. pallida</i>]
	SNP_85_126206	GPLIN_0003 82200	94832-100930	zinc finger protein	no	GROS_g1133 6	zinc finger protein [<i>Loa loa</i>]
		GPLIN_0003 82300	110433-110747	transcribed hypothetical protein	no		

	GPLIN_0003 82400	120748-122590	BTB:POZ domain containing protein 3	no	GROS_g1419 3	truncated secreted SPRY domain-containing protein 15, partial [<i>G. rostockiensis</i>]	
	GPLIN_0003 82500	126792-129853	SPIa RYanodine receptor SPRY	no	GROS_g1416 3	RBP-4 protein [<i>G. pallida</i>]	
	GPLIN_0003 82600	142203-143446	transcribed hypothetical protein	no			
	GPLIN_0003 82700	143942-144891	transcribed hypothetical protein	no			
	GPLIN_0003 82800	151467-154962	E9 protein	no	GROS_g1412 3	signal peptide	
	GPLIN_0003 82900	164278-168506	glutathione synthetase	no	GROS_g0539 0 / GROS_g1379 7	glutathione synthetase-like [<i>Maylandia zebra</i>] / glutathionesynthase; signal peptide	
	GPLIN_0003 83000	169444-172268	Guanine nucleotide binding protein G(o) subunit	no	GROS_g0538 9	guanine nucleotide-binding protein alpha-3 subunit [<i>Brugia malayi</i>]	
	GPLIN_0003 83100	174565-177704	ODR 3	no	GROS_g0538 9	guanine nucleotide-binding protein alpha-3 subunit [<i>B. malayi</i>]	
	GPLIN_0003 83200	179602-190327	guanine nucleotide exchange factor for Ras	no	GROS_g0538 8	regulation of Ral GTPase activity	
	GPLIN_0004 50000	79896-81897	UDP glucuronosyltransferase	yes	GROS_g0933 7	integral to plasma membrane	
	GPLIN_0004 50100	94652-95140	hypothetical protein	no			
	GPLIN_0004 50200	98715-99013	transcribed hypothetical protein	no			
	GPLIN_0004 50300	120569-121060	hypothetical protein	no			
	GPLIN_0004 50400	126241-129974	protein containing SPRY domain	no	GROS_g1419 5	dendrite morphogenesis, truncated secreted SPRY domain-containing protein 15, partial [<i>G. rostockiensis</i>]	
	GPLIN_0004 50500	132676-135723	inversin protein alternative, ankyrin repeat protein	no	GROS_g1419 2	protein binding	
111	SNP_111_ 140151	GPLIN_0004 50600	133821-134846	BTB:POZ domain containing protein 3	no	GROS_g1419 5	dendrite morphogenesis, truncated secreted SPRY domain-containing protein 15, partial [<i>G. rostockiensis</i>]
	GPLIN_0004 50700	138326-138779	transcribed hypothetical protein	no			
	GPLIN_0004 50800	138941-139562	Nematode AStacin protease family member	no	GROS_g0742 2	molting cycle, collagen and cuticulin-based cuticle; Astacin	
	GPLIN_0004 50900	144927-150255	NAD kinase domain containing protein 1	no	GROS_g1280 7 / GROS_g1280 8	NAD metabolic process / mRNA surveillance pathway	
	GPLIN_0004 51000	153798-155515	transcribed hypothetical protein	no			

	GPLIN_0004 51100	156162-159524	Amino Acid Transporter family member (aat 5)	no	GROS_g1280 5 / GROS_g0027 5	transmembrane transport / protein digestion and absorption	
	GPLIN_0004 51200	160262-161491	cyclin B	no	GROS_g0426 2	microtubule cytoskeleton	
	GPLIN_0004 51300	162184-162860	transcribed hypothetical protein	no	GROS_g0426 1	bifunctional 3 -phosphoadenosine 5 -phosphosulfate synthase [<i>Ascaris suum</i>]	
	GPLIN_0004 51400	163767-166872	serine:threonine protein phosphatase 5	no	GROS_g0426 0	transcription, DNA-dependent	
	GPLIN_0004 51500	168900-173567	transcribed hypothetical protein	no	GROS_g0425 8	protein binding	
	GPLIN_0004 51600	174095-175144	40S ribosomal protein S26	no	GROS_g0425 7	RNA metabolic process	
	GPLIN_0004 51700	175416-177669	transcribed hypothetical protein	no	GROS_g0425 6	transmembrane	
	GPLIN_0004 51800	177949-181975	DNA replication licensing factor MCM6	no	GROS_g0425 5	cell cycle - yeast	
	GPLIN_0004 51900	182477-187262	SWI:SNF complex subunit SMARCC2	no	GROS_g0425 4	ATP catabolic process	
	GPLIN_0004 52000	187774-189157	DNA replication complex GINS protein SLD5	no	GROS_g0425 3	nucleoplasm	
	GPLIN_0004 52100	192011-196045	transcribed hypothetical protein	no	GROS_g0425 2	transmembrane	
	GPLIN_0004 52200	197876-201179	transcribed hypothetical protein	no	GROS_g1089 1	galactosyl beta-1,3 N-acetylgalactosamine beta-1,3-glucuronosyltransferase activity	
	GPLIN_0004 82300	35198-37842	KH domain containing protein	no	GROS_g0608 4	nematode larval development; masculinization of hermaphroditic germ-line	
	GPLIN_0004 82400	59414-60834	transcribed hypothetical protein	no			
	GPLIN_0004 82500	61285-62959	nematode cuticle collagen N terminal domain	no	GROS_g1111 3	larval development ; transmembrane	
	GPLIN_0004 82600	72586-74133	transcribed hypothetical protein	yes			
123	SNP_ 123_ 97233	GPLIN_0004 82700	79061-79808	transcribed hypothetical protein	no	GROS_g1355 1	signal peptide
	GPLIN_0004 82800	85115-87297	mucosa associated lymphoid tissue lymphoma	no			
	GPLIN_0004 82900	87613-89268	mucosa associated lymphoid tissue lymphoma	no			
	GPLIN_0004 83000	89592-91491	mucosa associated lymphoid tissue lymphoma	no	GROS_g1111 7	ubiquitin-protein ligase activity; peptidase activity	
	GPLIN_0004 83100	98509-100826	sucrose hydrolase	no	GROS_g1137 4	beta-fructofuranosidase; signal peptide	

	GPLIN_0004 83200	101689-102752	tail length tape measure protein	no		
	GPLIN_0004 83300	103018-107209	beta fructofuranosidase; secreted GH32 fructosidase	yes	GROS_g1139 7	beta-fructofuranosidase; plant-type cell wall modification
	GPLIN_0004 83400	108777-111065	transcribed hypothetical protein	yes		
	GPLIN_0004 83500	112509-112790	transcribed hypothetical protein	no		
	GPLIN_0004 83600	117038-117476	transcribed hypothetical protein	yes		
	GPLIN_0004 83700	119298-120112	mps one binder kinase activator 3 like	no	GROS_g0971 1	neuronal cell body; perinuclear region of cytoplasm; microtubule cytoskeleton organization
	GPLIN_0004 83800	120304-121636	ubiquitin interacting motif	no	GROS_g0971 2	perinuclear region of cytoplasm
	GPLIN_0004 83900	121782-123696	ATP synthase subunit beta, mitochondrial	no	GROS_g0971 3	oxidative phosphorylation
	GPLIN_0004 84000	123896-127752	protein arginine N methyltransferase 5	no	GROS_g0971 4	protein ubiquitination; negative regulation of mitotic cell cycle
	GPLIN_0004 84100	128956-130197	tryptophanyl tRNA synthetase	no		
	GPLIN_0004 84200	137371-139503	transcribed hypothetical protein	no	GROS_g0970 7	transmembrane
	GPLIN_0004 84300	141658-142945	receptor type tyrosine protein phosphatase eta	no	GROS_g0503 2	protein tyrosine phosphatase activity; salicylic acid mediated signaling pathway
	GPLIN_0004 84400	148275-154307	transcribed hypothetical protein	no	GROS_g0502 8	glycerophospholipid metabolism; phosphatidylcholine metabolic process; signal peptide
	GPLIN_0004 84500	154735-155098	transcribed hypothetical protein	no		
	GPLIN_0004 84600	155919-159554	mitotic checkpoint serine:threonine protein	no	GROS_g0428 7 / GROS_g0502 7	regulation of chromosome segregation; positive regulation of intrinsic apoptotic signaling pathway / mitotic cell cycle spindle assembly checkpoint
	GPLIN_0006 26500	1034-2234	protein containing SPRY domain	no	GROS_g1424 1	regulation of Ran GTPase activity; RBP-1 protein [<i>G.pallida</i>]
SNP_182_414	GPLIN_0006 26600	4596-5610	transcribed hypothetical protein	no		
	GPLIN_0006 26700	9510-11116	protein containing SPRY domain	no	GROS_g1418 4	regulation of Ran GTPase activity; RBP-4 protein [<i>G.pallida</i>]
SNP_182_557	GPLIN_0006 26800	13854-21499	protein containing SPRY domain	no	GROS_g1419 6	cytoplasmic microtubule; RBP-4 protein [<i>G.pallida</i>]
	GPLIN_0006 26900	23491-25804	protein containing SPRY domain	no	GROS_g1419 5	truncated secreted SPRY domain-containing protein 15, partial [<i>G.rostochiensis</i>]
	GPLIN_0006 27000	27744-30562	transcribed hypothetical protein	no		

	GPLIN_0006 27100	41665-44164	paralog of RBP-1 protein	yes	GROS_g1425 6	ran GTPase binding; RBP-1 protein, partial [<i>G. pallida</i>]	
	GPLIN_0006 27200	45726-46823	60S acidic ribosomal protein P1	no	GROS_g0137 0	ribosome	
	GPLIN_0006 27300	49760-52726	transcribed hypothetical protein	no			
	GPLIN_0006 27400	55950-61422	serpin protein	yes	GROS_g0986 8	extracellular space	
<hr/>							
	GPLIN_0006 91700	593-1233	transcribed hypothetical protein	no			
	GPLIN_0006 91800	3867-5051	dorsal gland cell specific expression protein	no	GROS_g1429 8	dorsal gland cell-specific expression protein [<i>Heterodera avenae</i>]	
	GPLIN_0006 91900	9497-12258	mimitin, mitochondrial	no	GROS_g0527 4	NADH ubiquinone oxidoreductase subunit NDUFA12	
	GPLIN_0006 92000	13158-18286	succinyl CoA:3 ketoacid coenzyme A transferase	no	GROS_g0527 7 / GROS_g0248 7	butanoate metabolism / butanoate metabolism	
	GPLIN_0006 92100	18536-19094	histone cluster 2, H3c2	no	GROS_g0527 8	protein complex	
	GPLIN_0006 92200	19401-19965	H2A histone family, member X	no	GROS_g1075 6	positive regulation of DNA repair	
	GPLIN_0006 92300	21646-27499	transcribed hypothetical protein	no	GROS_g0203 4	small GTPase mediated signal transduction	
	GPLIN_0006 92400	27752-30375	transcribed hypothetical protein	no			
216	SNP_216_ 53947	GPLIN_0006 92500*	31556-57322	copine domain containing protein 2	no	GROS_g0203 2	plasma membrane
	GPLIN_0006 92600	57566-59215	transcribed hypothetical protein	no	GROS_g0203 2	plasma membrane	
	GPLIN_0006 92700	66169-72222	solute carrier family 23	no	GROS_g0203 1 / GROS_g0364 5	nucleobase transport / plasma membrane	
	GPLIN_0006 92800	78865-80575	serine:arginine rich splicing factor 4	no	GROS_g0203 0	mitosis	
	GPLIN_0006 92900	83168-85506	T complex protein 1 subunit gamma	no	GROS_g0202 8	extracellular vesicular exosome	
	GPLIN_0006 93000	85945-87738	T complex protein 1 subunit gamma	no	GROS_g0202 8	extracellular vesicular exosome	
	GPLIN_0006 93100	88182-90397	heterogeneous nuclear ribonucleoprotein A1	no	GROS_g0202 6	spliceosome	
	GPLIN_0006 93200	91404-93983	transcribed hypothetical protein	no	GROS_g0202 5	phosphatidylinositol-4,5-bisphosphate4-phosphatase.	

		GPLIN_0006 93300	95369-98967	transcribed hypothetical protein	no	GROS_g0202 4	plasmin
		GPLIN_0006 93400	100056-103180	nicotinic acetylcholine receptor non alpha	yes	GROS_g0202 2	response to inorganic substance
		GPLIN_0006 93500	104161-105279	transcribed hypothetical protein	no	GROS_g0202 1	hypothetical protein Y032_0018g3584 [<i>Ancylostoma ceylanicum</i>]
		GPLIN_0006 93600	105754-107423	bifunctional aminoacyl tRNA synthetase	no	GROS_g0202 0	porphyrin and chlorophyll metabolism
		GPLIN_0006 93700	107723-110938	u3 small nucleolar rna associated protein 14	no	GROS_g0201 9	ribosome biogenesis in eukaryotes
		GPLIN_0006 93800	111764-113032	succinate dehydrogenase cytochrome b560 subunit	no	GROS_g0201 8	defense response to Gram-negative bacterium
		GPLIN_0006 93900	113418-114209	'cold shock' DNA binding domain containing protein	no	GROS_g0201 7	sequence-specific DNA binding
		GPLIN_0008 14000*	56408-57804	BTB:POZ domain containing protein At1g55760	no		
		GPLIN_0008 14100	58370-60428	BTB:POZ domain containing protein At1g55760	no		
		GPLIN_0008 14200	61441-67930	transcribed hypothetical protein	yes	GROS_g1355 9	signal peptide
		GPLIN_0008 14300	68894-70678	BTB:POZ domain containing protein At1g55760	no		
	SNP_283_56739	GPLIN_0008 14400	72618-73953	transcribed hypothetical protein	no		
283		GPLIN_0008 14500	75558-76793	BTB:POZ domain containing protein At1g55760	no		
	SNP_283_56740	GPLIN_0008 14600	78642-79828	transcribed hypothetical protein	yes	GROS_g0578 8	signal peptide
		GPLIN_0008 14700	84623-91635	zinc metallopeptidase	no	GROS_g0578 9	metalloendopeptidase activity; peptidase family M13
		GPLIN_0008 14800	95043-97768	myelin transcription factor 1 protein	no	GROS_g1429 5	zinc finger, C2HC type
		GPLIN_0008 14900	107592-114130	transcribed hypothetical protein	no	GROS_g1421 3	BTB/POZ domain
		GPLIN_0008 15000	115751-116921	G patch domain containing protein	no		
		GPLIN_0008 32100**	6442-11746	Na:H eXchanger family member (nhx 9)	no	GROS_g0464 1 / GROS_g1341 8	protein F32B5.6, isoform j [<i>Caenorhabditis elegans</i>] / sodium:hydrogen antiporter activity
296	SNP_296_8846	GPLIN_0008 32200	12647-13096	transcribed hypothetical protein	no		
		GPLIN_0008 32300	17388-19554	transcribed hypothetical protein	no		

		GPLIN_0008 32400	33723-34555	transcribed hypothetical protein	no		
		GPLIN_0008 32500	35455-36989	transcribed hypothetical protein; Gpa_Dog_0189	yes		
		GPLIN_0008 32600	44182-46613	transcribed hypothetical protein	yes	GROS_g0830 7	lysosomal membrane
		GPLIN_0008 32700	47366-49673	lysosome associated membrane glycoprotein	yes	GROS_g0830 7	lysosomal membrane
		GPLIN_0008 32800	50657-51448	transcribed hypothetical protein	no	GROS_g0830 8	aminoacyl-tRNAhydrolase.
		GPLIN_0008 32900	52058-53243	14-3-3 protein	no	GROS_g0596 3 / GROS_g0830 9	neurotrophin signaling pathway / neurotrophin signaling pathway
		GPLIN_0008 33000	54914-56106	14-3-3 protein	no	GROS_g0596 3 / GROS_g0830 9	neurotrophin signaling pathway / neurotrophin signaling pathway
		GPLIN_0008 33100	63249-68201	calcium binding EGF domain containing protein	no	GROS_g0831 0	hypothetical protein Y032_0091g2492 [<i>Ancylostoma ceylanicum</i>]
		GPLIN_0009 03300	71992-78704	transcribed hypothetical protein	no		
		GPLIN_0009 03400	86045-87892	transcribed hypothetical protein	no	GROS_g0349 0	response to chitin
		GPLIN_0009 03500	89309-92938	serpentine receptor, class T family member	no	GROS_g0664 5	transmembrane
		GPLIN_0009 03600**	97414-99406	dorsal gland cell specific expression protein	no	GROS_g1414 6 / GROS_g1422 4	dorsal gland cell-specific expression protein [<i>Heterodera avenae</i>] / transmembrane; dorsal gland cell-specific expression protein [<i>H. avenae</i>]
338	SNP_338_ 98803	GPLIN_0009 03700	102236-103533	protein MICAL 3	no	GROS_g0815 7	LIM domain
		GPLIN_0009 03800	104125-104725	LIM domain containing protein	no		
		GPLIN_0009 03900	105988-106776	transcribed hypothetical protein	no		
		GPLIN_0009 04000	107274-107909	protein MICAL 3	no		
		GPLIN_0009 04100	108895-109595	transcribed hypothetical protein	no		
		GPLIN_0009 04700	24813-25894	transcribed hypothetical protein	no	GROS_g0802 5	SSF52540
340	SNP_ 340_ 56189	GPLIN_0009 04800	35241-37595	nematode astacin protease family member	no	GROS_g0703 5	extracellular region; metalloendopeptidase activity; Astacin-like metalloendopeptidase [<i>Strongyloides ratti</i>]

		GPLIN_0009 04900	37694-40604	peptidase M12A, astacin	no	GROS_g1291 9	astacin (peptidase family M12A)
		GPLIN_0009 05000	42995-45732	cell death protein 3	no	GROS_g1255 5	execution phase of apoptosis
		GPLIN_0009 05100**	53759-57940	transcribed hypothetical protein	no		
		GPLIN_0009 05200	75502-76417	transcribed hypothetical protein	no		
						GROS_g1133 6 /	
		GPLIN_0009 14300	13395-18410	zinc finger protein 280D	no	GROS_g0245 0 /	zinc finger protein [<i>L. loa</i>] / signal peptide / zinc finger C2H2 type domain signature
349	SNP_349_ 8349	GPLIN_0009 14400	31215-32425	transcribed hypothetical protein	no	GROS_g1122 3	
		GPLIN_0009 14500	63737-66258	transcribed hypothetical protein	no	GROS_g1005 8	signal peptide
		GPLIN_0009 14600	69418-70547	ubiquitin carboxyl terminal hydrolase 48	no	GROS_g0335 6	ubiquitinylhydrolase1
		GPLIN_0010 56200	3568-10018	transcribed hypothetical protein	no	GROS_g1153 8	zinc finger C2H2 type domain signature.
		GPLIN_0010 56300	10515-10989	transcribed hypothetical protein	no	GROS_g1153 9	transmembrane
		GPLIN_0010 56400	11106-12182	transcribed hypothetical protein	yes	GROS_g1153 9	transmembrane
		GPLIN_0010 56500	13710-14450	transcribed hypothetical protein	no		
474	SNP_ 474_ 28528	GPLIN_0010 56600	14570-20232	transcribed hypothetical protein	no	GROS_g1154 0	signal peptide
		GPLIN_0010 56700	52073-52540	transcribed hypothetical protein; Gpa_Dog_0074	yes		
		GPLIN_0010 56800	56482-58809	transcribed hypothetical protein	no		
		GPLIN_0010 56900	58931-60252	transcribed hypothetical protein	yes		
		GPLIN_0010 57000	62667-67109	transcribed hypothetical protein	no		
		GPLIN_0010 82800	211-620	protein containing SPRY domain	no	GROS_g1416 3	RBP-4 protein [<i>G. pallida</i>]
504	SNP_ 504_ 47039	GPLIN_0010 82900	11855-12808	paralog of RBP-5 protein (33H17)	no	GROS_g1417 9	RBP-1 [<i>G. pallida</i>]; signal peptide
		GPLIN_0010 83000	14667-16919	transcribed hypothetical protein	yes	GROS_g1300 8	hypothetical protein TcasGA2_TC001495 [<i>Tribolium castaneum</i>]

		GPLIN_0010 83100	18255-23950	transcribed hypothetical protein	yes	GROS_g1045 6	thap domain-containing protein 4 [<i>A. suum</i>]; transmembrane
		GPLIN_0010 83200	25548-26905	transcribed hypothetical protein	no		
		GPLIN_0010 83300	32640-39130	serine:threonine protein kinase SIK3	no	GROS_g1045 4	serine threonine-protein kinase kin-29 [<i>A. suum</i>]
		GPLIN_0010 83400*	43996-50149	3 hydroxy 3 methylglutaryl coenzyme A reductase	no	GROS_g1045 2	hmg CoA reductase A [<i>Polysphondylium pallidum</i> PN500]; protein homodimerization activity
		GPLIN_0010 83500	54107-59069	transcribed hypothetical protein	no	GROS_g1045 1	peptidase M10A M12B domain containing protein [<i>H. contortus</i>]; transmembrane; matrixin
		GPLIN_0012 57900	8259-9831	transcribed hypothetical protein	no	GROS_g1414 6	dorsal gland cell-specific expression protein [<i>H. avenae</i>]; putative esophageal gland cell protein Hgg-20 [<i>H. glycines</i>]
		GPLIN_0012 58000	16237-17191	transcribed hypothetical protein	no	GROS_g1421 3	BTB/POZ domain
782	SNP_ 782_ 20136	GPLIN_0012 58100**	19137-20558	paralog of RBP-1 protein; Gpa_Dog_0077	yes	GROS_g1423 4	RBP-1 protein [<i>G. pallida</i>]; secreted SPRY domain- containing protein 16, partial [<i>G. rostochiensis</i>]
		GPLIN_0012 58200	25107-27756	ubiquitin 40S ribosomal protein S27a 1	no	GROS_g0756 8	protein ubiquitination
		GPLIN_0012 58300	31187-31435	transcribed hypothetical protein	no		
		GPLIN_0012 58400	33199-34624	protein containing SPRY domain	no	GROS_g1418 4	RBP-4 protein [<i>G. pallida</i>]; secreted SPRY domain- containing protein 9 [<i>G. rostochiensis</i>]
	SNP_ 988_ 7923	GPLIN_0013 23400	2535-3808	transcribed hypothetical protein	no	GROS_g0156 8	protein of unknown function, DUF273
		GPLIN_0013 23500	12021-16917	serine:threonine protein kinase Nek6	no	GROS_g0133 4	serine/threonine-protein kinase Nek6, partial [<i>Bos mutus</i>]; cytokinesis; signal transducer activity
988	SNP_ 988_ 8037	GPLIN_0013 23600	19109-26588	Motor AXon guidance family member (max 2)	no	GROS_g1007 7	protein BM-MAX-2, isoform i [<i>B. malayi</i>]; K04409 Axon guidance
	SNP_ 988_ 8045						
	SNP_ 988_ 8100						
1243	SNP_1243 9865			no predicted gene			
		GPLIN_0014 38500**	864-1181	transcribed hypothetical protein	no		
1777	SNP_1777 961	GPLIN_0014 38600	2326-4922	maternal protein pumilio	no	GROS_g1428 6	cytosol
		GPLIN_0014	6616-7313	transcriptional regulator ATRX	no		

38700

3221	SNP_3221 _1475	GPLIN_0015 18200	1511-2451	dorsal gland cell specific expression protein	no	GROS_g1414 3 / GROS_g1413 9	transmembrane; dorsal gland cell-specific expression protein [<i>H. avenae</i>] / transmembrane; dorsal gland cell-specific expression protein [<i>H. avenae</i>]
3816	SNP_3816 _941				no predicted gene		
5159	SNP_5159 _970				no predicted gene		

811